# Circadian clock-coordinated 12 Hr period rhythmic activation of the IRE1α pathway controls lipid metabolism in mouse liver

Gaspard Cretenet[1, 2], Mikaël Le Clech[1] and Frédéric Gachon[1, 2]

[1] Institut de Génétique Humaine; CNRS UPR 1142; Montpellier, F-34396, France

[2] Present address: Department of Pharmacology and Toxicology, University of Lausanne, Lausanne, CH-1005, Switzerland

**Contact:**

Frédéric Gachon
University of Lausanne
Department of Pharmacology and Toxicology
Rue du Bugnon, 27
CH-1005 Lausanne
Switzerland

Tel: (00 41) 21 692 53 64
Fax: (00 41) 21 692 53 55

E-mail: Frederic.Gachon@unil.ch

**Running title:** Rhythmic activation of the IRE1α pathway

## Summary

The mammalian circadian clock plays a fundamental role in the liver by regulating fatty acid, glucose and xenobiotic metabolism. Impairment of this rhythm has been shown to lead to diverse pathologies including metabolic syndrome. Currently, it is supposed that the circadian clock regulates metabolism mostly by regulating expression of liver enzymes at the transcriptional level. Here we show that the circadian clock controls also hepatic metabolism by synchronizing a secondary 12-hours period rhythm characterized by rhythmic activation of the IRE1α pathway in the endoplasmic reticulum. The absence of circadian clock perturbs this secondary clock and provokes deregulation of endoplasmic reticulum-localized enzymes. This leads to impaired lipid metabolism conducting to aberrant activation of the sterol regulated SREBP transcription factors. The resulting aberrant circadian lipid metabolism in mice devoid of clock could be involved in the appearance of the associated metabolic syndrome.

## Introduction

Circadian clocks have been conserved throughout evolution to allow anticipation of physiology and behaviour of the organisms to the environmental changes. As a consequence, most aspects of animal metabolism are under the control of this molecular oscillator (Green et al., 2008). Current models suggest that the circadian clock regulates metabolism mainly at the transcriptional level. Indeed, the heterodimer composed of BMAL1 and its partners CLOCK or NPAS2 is a transcriptional activator which regulates transcription of the *Period* (*Per*) and *Cryptochrome* (*Cry*) genes that code for repressors of BMAL1 heterodimer activity, thus controlling a negative feedback loop that generates these rhythms of approximately 24 hours (Gallego and Virshup, 2007).

The endoplasmic reticulum (ER) is a sophisticated luminal network in which protein synthesis, maturation, folding, and transport take place (Marciniak and Ron, 2006; Schröder and Kaufman, 2005). Interestingly, many enzymes involved in mammalian liver metabolism are localized in the ER membrane of hepatocytes. It has been previously described that in these cells ER exhibits a circadian dilatation which is a sign of ER stress (Chedid and Nair, 1972). This stress triggers the unfolded protein response (UPR) which is a universally conserved adaptative response to cope with the accumulation of unfolded proteins in this organelle. When unfolded proteins accumulate in ER, three pathways are activated, IRE1$\alpha$, PERK and ATF6, which lead to the nuclear translocation of the transcription factors XBP1, ATF4 and ATF6, respectively. These transcription factors activate in turn the expression of genes coding for proteins involved in peptide folding and degradation to limit the accumulation unfolded proteins. In the case this is not sufficient, UPR ultimately leads to apoptosis to preserve the organism (Ron and Walter, 2007).

Recent studies show that UPR could also function as a regulator of hepatic lipid metabolism through either a direct transcriptional control of genes coding for proteins involved in lipid metabolism or by interfering with the secretion of apolipoproteins (Lee and Glimcher, 2009). As many aspects of hepatic lipid metabolism are

also under the control of the circadian clock, we decided to determine if there exists a link between activation of the UPR and the circadian clock. Here we show that all the UPR-regulated genes tested showed a rhythmic expression according to an apparent 12-hours period dependent on a functional circadian clock. This rhythmic activation of UPR regulated genes seems to be the consequence of the activation of the IRE1α-XBP1 pathway which is activated according to the same 12-hours period rhythm. As a consequence, mice lacking a functional circadian clock show flattened rhythm of IRE1α pathway activation which leads to deregulation of ER resident enzymes and to perturbed lipid metabolism.

## Results

### Rhythmic response to ER stress-inducing agent

To characterise a possible time-dependent response to ER stress-inducing agent, mice were injected i.p. every 4 hours with Tunicamycin, an inhibitor of glycosylation that induces UPR, and sacrificed 4 hours after the injection. By western blotting, we evaluated the activation state of the UPR activated transcription factors and noticed a strong activation of the three UPR pathways (Figure 1A). p90-ATF6α degradation seems to be more important when Tunicamycin is injected between ZT6 and ZT18 but we were not able to detect the nuclear activated p50-ATF6α probably due to the strong instability of this form (Thuerauf et al., 2002). ATF4 translation reached its maximum when Tunicamycin is injected between ZT22 and ZT6. Finally, XBP1 activation presented a more complex pattern with two peaks, one at ZT2 and another between ZT10 and ZT18. Interestingly, induction of the UPR activated transcription factor CHOP (Wang et al., 1996) followed exactly the same profile. IRE1α is a ribonuclease processing *Xbp1* mRNA, resulting in the expression of the potent activating transcription factor XBP1 (Calfon et al., 2002; Lee et al., 2002; Yoshida et al., 2001). Splicing of *Xbp1* mRNA presented the same bimodal profile whereas no change was found for

the total *Xbp1* mRNA (Figure 1B). Concomitantly, induction of the mRNA coded by the UPR regulated genes *Bip* and *Chop* followed also the same bimodal profile (Figure 1C).

Overexpression of ER-resident Cytochrome P450 enzymes has been linked to induction of UPR (Szczesna-Skorupa et al., 2004) and Tunicamycin was shown to induce *Cyp2b10* expression at the same extent as Phenobarbital (Rutkowski et al., 2008). In addition, response to xenobiotics is regulated by the circadian clock (Gachon et al., 2006). Therefore, it is possible that rhythmic induction of Cytochrome P450 enzymes could generate the observed activation of the UPR. However, induction of *Cyp2b1*0 by Tunicamycin presented a clear diurnal pattern, with maximal induction between ZT10 and ZT18 (Figure 1D) which could thus not explain the complex pattern of XBP1 activation.

Since activation of the UPR has been recently linked to lipid metabolism (Lee et al., 2008; Ota et al., 2008; Rutkowski et al., 2008), we measured serum and liver concentrations of triglycerides and cholesterol after injection of Tunicamycin. As shown in Figure 1E and Figure S1, we found a strong decrease in serum concentration of triglycerides and cholesterol and a high increase of triglycerides concentration in the liver after Tunicamycin injection. However, these changes did not seem to depend on the time of injection. According to previously published data, these lipid metabolic changes could be explained by both decreased lipogenesis (Lee et al., 2008; Rutkowski et al., 2008) and inhibition of apolipoprotein B100 secretion (Ota et al., 2008).

XBP1 is also known to regulate a subset of genes involved in ER associated degradation (ERAD) (Yoshida et al., 2003), a process involved in the elimination of unfolded proteins inside ER (Meusser et al., 2005). Enzymes involved in cholesterol or fatty acid metabolism localized inside the ER membrane present low half-lives due to their sensitivity to ERAD. This is for example the case for HMG-CoA Reductase (HMGCR), the rate limiting enzyme of cholesterol synthesis (Hampton, 2002) and Stearoyl-CoA Desaturase 1 (SCD1), which is involved in the synthesis of unsaturated fatty acids (Kato et al., 2006). In addition, IRE1α activation causes not only processing of *Xbp1* mRNA but also endonucleolytic decay of many ER-

localized mRNA both in *Drosophila* (Hollien and Weissman, 2006) and in mammalian cells (Han et al., 2009; Hollien et al., 2009), including *Hmgcr* mRNA. Elsewhere, Tunicamycin has been shown to strongly inhibit HMGCR activity in cultured cells (Volpe and Goldberg, 1983). Therefore, we studied the consequences of Tunicamycin injection on HMGCR and SCD1 expressions as well as Fatty acid synthase (FASN) which is ERAD insensitive. As shown on Figure 1F, Tunicamycin induced a strong decrease in the abundance of HMGCR and SCD1 whereas no effect was seen on FASN expression. Interestingly, this effect seems to be synchronized with XBP1 activation, especially in the case of SCD1. Degradation of ER-localized enzymes through ERAD could thus be also involved in the deregulated lipid metabolism associated with UPR activation.

**Rhythmic activation of the IRE1α pathway in mouse liver**

We noticed in control mice a lower magnitude biphasic rhythmic splicing of *Xbp1* mRNA. To characterize the possible rhythmic activation of the UPR in mouse liver in standard laboratory conditions, we measured the temporal expression of well-known UPR activated genes. Surprisingly, all the UPR-regulated genes tested showed a rhythmic expression, not according to a 24-hours period, but rather to the same apparent biphasic 12-hours period with two unsymmetrical peaks at ZT2 and ZT14-16 (Figure 2A Figure S2). This behaviour is in agreement with recent results showing hundreds of 12-hours period rhythmically expressed genes including UPR regulated genes (Hughes et al., 2009). Among the three pathways activated during the UPR, only the IRE1α pathway presented a rhythmic activation characterized by the biphasic phosphorylation of the protein (Figure 2B). The reverse rhythmic patterns of the total protein and mRNA levels was probably due to the fact that activated IRE1α is able to cut is own mRNA (Tirasophon et al., 2000) leading then to a lower total protein amount (Figures 2B and 2C). According to the IRE1α activation, we found a rhythmic accumulation of the processed *Xbp1* mRNA (Figure 2D) whereas total *Xbp1* mRNA

appeared non-rhythmic (Figure S3A). As a consequence, we observed a biphasic nuclear accumulation of the XBP1 transcription factor matching the rhythmic phosphorylation of IRE1α (Figure 2E). This rhythmic activation of the IRE1α-XBP1 pathway could explain the observed rhythmic ER dilation as XBP1 has been linked to ER expansion through activation of membranes biosynthesis (Sriburi et al., 2004).

**12-hours period rhythmic activation of the IRE1α pathway is preserved in the absence of light or food**

One characteristic of circadian rhythms is the fact that they are self-sustained and maintained under constant conditions. Therefore we tested whether these 12-hours period rhythms persisted in constant darkness and found that rhythmic phosphorylation of IRE1α, processing of *Xbp1* mRNA and nuclear accumulation of XBP1 are preserved under these conditions (Figure 3A).

After light, the major *Zeitgeber* for the circadian clock is food which is being even considered as the major regulator of peripheral clocks (Damiola et al., 2000). Hence, we studied the effect of food deprivation on the biphasic activation of the UPR in mouse liver. After a complete night of fasting, livers were harvested every two hours for the next 22 hours. As shown in Figure 3B, rhythmic phosphorylation of IRE1α and processing of *Xbp1* mRNA were maintained under this condition. The disturbed accumulation of the XBP1 protein could be explained by the inhibition of cap-mediated translation during starvation (Kimball and Jefferson, 1994).

**Rhythmic activation of the IRE1α pathway is linked to circadian clock-controlled rhythmic lipid metabolism**

It has been recently shown that UPR is induced by feeding (Oyadomari et al., 2008), and more particularly by high fructose (Lee et al., 2008) or high fat diets (Ozcan et al., 2004). This could explain why some of the 12-hours period expressed genes could be entrained by changes in the feeding schedule (Hughes et al.,

2009). To define more precisely the impact of food on UPR activation, mice were fed after 12 hours of starvation with normal, high fat or fat free (high sucrose) diets. Whereas normal diet induced a transient activation of XBP1, high fat diet induced a sustained activation and fat-free diet caused a delayed activation that correlated with the start of *de novo* synthesis of fatty acid induced by ChREBP activation (Uyeda and Repa, 2006) (Figure S4). Circadian clock-regulated lipid metabolism could then be a major regulator of this 12-hours period rhythmic activation of IRE1α. In addition, excess of fatty acid or cholesterol induces UPR (Feng et al., 2003; Ozcan et al., 2004), as well as deficiencies in *de novo* fatty acid synthesis in the liver (Flowers et al., 2008; Little et al., 2007). With respect to lipid excess, we speculated that obesity could potentially interfere with the rhythmic activation of IRE1α. As shown in Figure S5, IRE1α was strongly phosphorylated throughout the day in the liver of *ob*/*ob* mice. However, the rhythm of phosphorylation was comparable to the one found in wild-type mice, albeit with lower amplitude. Thus, even if obesity seems to play a role in the magnitude of IRE1α activation, it does not seem to interfere with its periodicity.

We have recently shown that many aspects of lipid metabolism are regulated by PARbZip proteins, a family of circadian clock-regulated transcription factors involved in the regulation of clock output pathways (Gachon, 2007). Indeed, in PARbZip deficient mice, the biphasic liver fatty acid metabolism orchestrated by acyl-CoA thioesterases and lipoprotein lipase is strongly altered and replaced by an increased *de novo* synthesis through induction of FASN (FG et al., submitted manuscript). As a consequence, the 12-hours period rhythmic activation of XBP1 is replaced by an apparent 24-hours period which correlated with a 24-hours period expression of UPR regulated genes (Figure 4A). We also studied the rhythmic activation of the IRE1α in *Clock* knockout (ko) mice. These mice have a robust circadian behavior but a lower expression of some clock-controlled genes in peripheral tissue, including the PARbZip transcription factor *Dbp* (DeBruyne et al., 2006). Interestingly, they exhibit a change in the rhythm of activation of IRE1α which is very similar to PARbZip triple ko mice (Figure S6).

To confirm the implication of the circadian clock in the 12-hours period rhythmic IRE1α activation, we studied it in mice deleted for the two *Cry* genes. *Cry1*/*Cry2* ko mice show an arrhythmic pattern of activity under constant darkness and constant average levels of PARbZip genes expression (van der Horst et al., 1999). This arrhythmic behaviour of locomotor activity is in general correlated with an arrhythmic feeding behaviour. As UPR is activated by feeding, we would expect a stochastic activation of this pathway in *Cry1*/*Cry2* ko mice kept in constant darkness. To explore this possibility, six *Cry1*/*Cry2* ko mice were kept in constant darkness during one week and sacrificed at CT12. Under these conditions, we observed a stochastic activation of the splicing of *Xbp1* mRNA correlated with a random accumulation of nuclear XBP1 and expression of its target genes (Figure S7). To circumvent this problem, we placed *Cry1*/*Cry2* ko mice under a light-dark regimen to maintain a normal diurnal feeding behaviour due to masking. We found under this condition a sustained phosphorylation of IRE1α while the processing of *Xbp1* mRNA appeared elevated throughout the time with a peak at ZT10-14 when animals start eating (Figure 4B). The nuclear accumulation of XBP1 followed the same pattern whereas the consequential expression of UPR-regulated genes showed a quasi-24-hours period profile with high mRNA levels between ZT10 and ZT18.

**Constitutive activation of the IRE1α pathway in *Cry1*/*Cry2* ko mice leads to perturbed lipid metabolism**

As a consequence of the constant activation of the IRE1α pathway, *Cry1*/*Cry2* ko mice expressed XBP1 target genes during a longer period than wild-type mice. This resulted in their higher overall expression, as well as higher IRE1α endonucleotic activity. As shown in Figure 5A, diurnal expression of HMGCR strongly decreased in *Cry1/Cry2* ko, coinciding with its very low level of expression. In addition, rhythmic accumulation of SCD1 was perturbed while its overall level significantly decreased. It is interesting to note that the level of HMGCR and SCD1 in wild-type mice is lower at ZT2 and between ZT12-16 (Figure 5A)

when XBP1 exhibits its maximum of expression (Figure 2A). However, the abundance of FASN did not decrease and its abundance is in agreement with its mRNA level (see below).

Perturbed HMGCR and SCD1 levels were not a consequences of decreased transcription since their mRNA levels did not diminish in *Cry1*/*Cry2* ko mice (Figure 5B). However, the rhythmic expression pattern of these genes was dramatically altered, shifting from one peak of expression at ZT18-20 to two peaks at ZT4-6 and 16-18. All these genes, including *Fasn* which exhibit the same expression pattern, are mostly regulated by the Sterol Responsive Element Binding Protein (SREBP) transcription factor (Horton et al., 2003). SREBP is an ER membrane bond protein that, in low sterol conditions, translocates to the Golgi to be cleaved and released in order to migrate in the nucleus where it activates genes coding for enzymes involved in cholesterol and fatty acid metabolism (Espenshade and Hughes, 2007). Interestingly, ER stress induces cleavage and activation of SREBP1 and SREBP2 (Colgan et al., 2007; Wang et al., 2005) through induced depletion of INSIG regulatory proteins (Bobrovnikova-Marjon et al., 2008; Lee and Ye, 2004). We therefore explored the rhythmic maturation of SREBP in *Cry1/Cry2* ko mice to study its implication in rhythmic expression of *Hmgcr*, *Scd1* and *Fasn*. We indeed found that in these mice SREBP1 and SREBP2 nuclear accumulation became biphasic with, in addition, an increased overall activation of SREBP2 (Figure 5C). This activation correlates with decreased levels of INSIG proteins, although this alone could not explain the rhythm of SREBP activation. This change in SREBP activity could not be explained by an increased transcription of *Srebp1* and *Srebp2* mRNA or a decreased transcription of *Insig1* and *Insig2* mRNA (Figure 5D), but their rhythms of expression are modified. Namely, *Srebp1* and *Insig1* seem to be more expressed at ZT2-6 like other SREBP target genes whereas the diurnal expression *Srebp2* and *Insig2* seems to be flattened due to their regulation by the circadian clock (Le Martelot et al., 2009; Miller et al., 2007). However, increased and bimodal SREBP activity seems to be rather due to a change in its maturation.

As cholesterol level is the main regulator of SREBP processing, we measured lipids concentrations in serum and liver of *Cry1*/*Cry2* ko mice. As shown in Figure S8, serum and liver cholesterol concentrations were not

different between wild-type and *Cry1*/*Cry2* ko mice, indicating that alteration of SREBP activation could not be explained by cholesterol concentration. However, we noticed an important change in triglycerides concentrations, with a decreased concentration in the serum and an increased concentration in the liver (Figure 5E). Theses changes were similar to those found after injection of Tunicamycin (Figure 1E) as previously described (Rutkowski et al., 2008). It has been shown that chemical chaperones correct the obesity-induced activation of UPR in mouse liver and decreased liver steatosis in *ob*/*ob* mice (Ozcan et al., 2006), probably by re-establishing a normal secretion of apolipoprotein B100 (Ota et al., 2008). We thus injected daily during two weeks one of this chemical chaperone, Tauroursodeoxycholic acid (TUDCA), and monitored its effect on triglycerides level in *Cry1*/*Cry2* ko mice. As shown on Figure 5E and Figure S8, TUDCA treatment corrected hepatic steatosis in *Cry1*/*Cry2* ko mice giving rise to liver triglycerides concentration that is equivalent with the one of wild-type mice. However, this did not affect serum triglycerides content, as described for obese mice (Ozcan et al., 2006). Serum and liver cholesterol concentrations were not changed. This data clearly suggests that the defect in triglycerides metabolism in *Cry1*/*Cry2* ko mice is the consequence of the constitutive activation of the UPR in the liver of these animals.

**12-hours period rhythmic IRE1α activation and diurnal SREBP maturation are coordinated by the circadian clock**

Next, we wished to determine whether the shifts of the IRE1α activation from 12-hours period to 24-hours period and the expression of SREBP target genes from 24-hours period to 12-hours period are due to the deletion of *Cry* genes or the consequence of an impaired molecular clock. To this end, we analyzed expression of their target genes in *ClockΔ19* mutant mice characterized by a dominant negative mutation in the *Clock* gene which caused their arrhythmic behaviour in constant darkness (King et al., 1997; Vitaterna et al., 1994). *Post-hoc* analysis of recently published microarray data (Miller et al., 2007) revealed that the

UPR regulated genes *Chop* and *Dnajb9* were expressed according to the same 12-hours period rhythm in the liver of control mice but exhibited a constant expression in *ClockΔ19* mice (Figure S9A). Similarly, all analyzed SREBP target genes shifted their apparent circadian expressions to a biphasic 12-hours period expression (Figure S9B). These results were validated by quantitative RT-PCR on liver RNA harvested every two hours during 24 hours from independent sets of wild-type and *ClockΔ19* mice. As shown on Figure 6, we found very low and constant splicing of *Xbp1* mRNA in *ClockΔ19* mice in comparison to the biphasic pattern obtained for wild-type mice, whereas no significant differences were found for total *Xbp1* mRNA. We also confirmed the low and constant expression of *Chop* and *Bip* mRNA. Finally, in contrast to wild-type mice, *ClockΔ19* mice exhibit a low level of expression of SREBP target genes with an apparent low amplitude biphasic rhythm, thus confirming the results obtained by *post-hoc* analysis of microarray data. Taken together, these results imply that the rhythmic liver lipid metabolism controlled by the circadian clock acts as a biphasic activator of the UPR.

## Discussion

### Rhythmic activation of the UPR in mouse liver

The main function of the circadian clock is to activate physiological processes within appropriate time windows by driving the cyclic expression and/or activity of implicated enzymes. In organs associated with the digestive tract, such as the liver, a major task of the circadian timing system is to adapt the metabolism to daily feeding-fasting rhythms. On the other hand, feeding-fasting cycles are dominant *Zeitgebers* for such organs (Damiola et al., 2000). Here we show a circadian-clock dependent rhythmic activation of the IRE1α-XBP1 pathway in the liver with a 12-hours period. Interestingly, activation of this pathway by Tunicamycin follows the same rhythm. Tunicamycin inhibits *N*-linked glycosylation of proteins by competing with UDP-

*N*-acetylglucosamine (UDPGlcNAc) for the enzyme UDPGlcNAc:dolichyl phosphate, *N*-acetylglucosamine-1-phosphate transferase (DPAGT1), the first enzyme of the dolichol cycle required for the process of *N*-linked glycosylation. Tunicamycin presents high structure homology with UDPGlcNAc and binds to DPAGT1 with approximately 200-fold more affinity (Keller et al., 2002). We can thus speculate that the two compounds could be transported *via* the same transporter located in the ER and Golgi. This transporter, SLC35D2 (Sesma et al., 2009), was found to be expressed according to a 12-hours cycle in mouse liver (Hughes et al., 2009). It is then possible that the rhythmic expression of the UDPGlcNAc transporter is also responsible of the rhythmic activation of the UPR by Tunicamycin. In addition, UDP-*N*-Acetylglucosamine Pyrophosphorylases (UAP1), the enzyme involved in the last step of UDPGlcNAc synthesis (Mio et al., 1998) has also been described to be expressed according with this 12-hours rhythm (Hughes et al., 2009). As a consequence, the synthesis and the transport of UDPGlcNAc could be both controlled by this 12-hours rhythm. Hence, the rhythmic abundance of UDPGlcNAc could explain the rhythmic response to Tunicamycin. It could also potentially produce a rhythmic *N*-linked glycosylation which can influence proteins transport outside the ER, therefore contributing to the rhythmic activation of UPR in mouse liver.

Other cases of synchronized rhythmic expression and induction have been described. For example, expression of *Cyp2b10* is synchronized to its rhythmic induction by Phenobarbital through Constitutive Androstane Receptor (CAR) activation (Gachon et al., 2006). The same observation has been made for the basal (Huang et al., 2002) and inducible expression of *Cyp1a1* and *Cyp1b1* genes by dioxin through activation of the Aryl Hydrocarbon Receptor (AHR) (Qu et al., 2007). Considering the fact that the main function of the circadian clock is to anticipate changes in the environment, it should not be surprising that the clock controls both the expression of the enzymes and the factors required for a rapid and massive response to intoxication. It is thus possible that the synchronized expression and Tunicamycin-dependent induction of UPR target genes belong to the same phenomenon.

**Implication of rhythmic activation of IRE1α pathway in hepatic lipid metabolism**

Our data imply that the IRE1α-XBP1 pathway is an important element of the circadian clock-regulated mouse hepatic lipid metabolism. Although previous work implicated XBP1 in fatty acid and cholesterol metabolisms, that control was only at the transcriptional level (Lee et al., 2008). We demonstrated here that this regulation involves also post-translational regulation likely through controlled degradation of ER resident enzymes like HMGCR and SCD1. Moreover, as lipid synthesis controls UPR induction, it is conceivable that its rhythmic activation by XBP1 could act as a second inducer, which stimulates and sustains a secondary 12-hours period metabolic clock in the liver (Figure 7). It is interesting to note that feeding acts as both an inducer of UPR target genes and a synchronizer of the liver clock. Considering the growing implication of the circadian clock on liver metabolism, we established here a link between circadian clock-controlled feeding behaviour, hepatic transformations of the metabolites and metabolites-dependent activation of the UPR which itself influences lipid metabolism. The interconnection between these different loops of regulation appears to be required for a proper liver metabolism. Indeed, the data presented here show that molecular circadian clock-deficient *Cry1*/*Cry2* ko mice present a perturbed rhythmic activation of the UPR in the liver inducing a lipid steatosis which is corrected by TUDCA treatment.

The disruption of this metabolites-controlled rhythm in circadian clock deficient mutant mice leads simultaneously to the strong reduction of the amplitude of 12-hours period rhythms and to the 12-hours period expression of SREBP target genes, probably caused by the disrupted sterol circadian metabolism in the liver. This second peak of SREBP target genes expression provokes an overall increase of their mRNA levels whereas the increased UPR activation maintained their protein products to low levels. As a consequence, uncoordinated levels of mRNA and protein for enzymes involved in fatty acids and cholesterol metabolism could participate in the disturbed lipid metabolism observed circadian clock deficient mice.

**Significance of 12 hours period rhythm in mouse liver**

We show here that the molecular circadian clock is involved in the rhythmic activation of the UPR with a 12 hours period in mouse liver. However, the two peaks of activation are not symmetrical with a small peak in the beginning of the day and a broader peak in the beginning of the night. Hypothetically, these two peaks could represent the superposition of two circadian peaks whose phases are separated by 12 hours. As activation of the UPR could be caused by different metabolic inducers, it is possible that the circadian clock driven hepatic metabolism creates conditions of activation of the UPR at different time point during the day. The goal of this manoeuvre could be the facilitation of ER-localized biochemical events that take place at different times. For example, during the night, Insulin stimulates the uptake of excess blood glucose and its conversion to glycogen by liver and muscle whereas during the day glucagon enhances glycogenolysis and gluconeogenesis when blood glucose levels fall (Cherrington et al., 1987). Interestingly, both phenomena are linked to expansion of the ER, a sign of ER stress (De Man et al., 1966; Morgan and Jersild, 1970). In addition, glycogen accumulation in models of defective glycogenolysis and gluconeogenesis is linked to induction of ER stress (Kim et al., 2008), as in the case of both prolonged hyperglycemia (Lindenmeyer et al., 2008) and hypoglycemia (Gonzales et al., 2008). Moreover, induction of ER stress stimulates glucose production and glycogen depletion through activation of Glycogen Phosphorylase (Gill et al., 2002; Gonzales et al., 2008). This suggests that induction of ER stress could be required to facilitate both reactions that are separated by 12 hours, at two different phases of the animal metabolic cycle.

We don't know yet if other examples of 12 hours separated biochemical events exists in animals. However, it has been recently shown that the coenzyme Nicotinamide Adenine Dinucleotide ($NAD^+$) is synthesized according to a circadian clock regulated 12 hours cycle in mouse liver (Ramsey et al., 2009). According to the central role of this biological cofactor, the rhythmic production of $NAD^+$ may have a cascade of effects on downstream pathways, including metabolism and aging, in part through the regulation of the $NAD^+$-dependent deacetylase SIRT1 (Blander and Guarente, 2004). Circadian-clock regulated 12-hours period

synthesis of metabolite may thus affect pathways other than UPR which can modulate animal metabolism. Interestingly, ultradian respiratory cycles have been shown to generate rhythmic expression of genes and accumulation of metabolites in budding yeast (Tu et al., 2005; Tu et al., 2007). These cycles are crucial as yeasts which have lost the capacity to sustain metabolic cycles present a high rate of DNA mutations (Chen et al., 2007). By analogy, perturbations of these 12-hours period metabolic rhythms could thus play an important role in metabolic syndromes that appeared in *Clock∆19* mutant mice feeding a high fat diet (Turek et al., 2005) or in human with perturbed circadian rhythms (Prasai et al., 2008; Scheer et al., 2009).

## Experimental Procedures

### Animal experiments

8 weeks male C57Bl/6J and C57Bl/6J-ob (*ob*/*ob*) mice were purchased from Janvier (Le Genest, France). Knockout mice for the three genes *Dbp*, *Hlf* and *Tef* coding for the PARbZip transcription factors have been previously described (Gachon et al., 2004). *Cry1*/*Cry2* double knockout mice (van der Horst et al., 1999) were backcrossed 10 times on C57Bl/6J to allow comparison of mice under the same genetic background (Bur et al., 2009). *Clock* knockout (DeBruyne et al., 2006) and *Clock∆19* mutant (Vitaterna et al., 1994) mice under the C57Bl/6J background have been previously described. Unless noted otherwise, mice were maintained under standard animal housing conditions, with free access to food and water and a 12h light/12h dark cycle. In all experiments, male mice between 10 and 12 weeks of age are used. All animal studies protocols were approved by our regional committee for ethics in animal experimentation. The details of the experiments are given in Supplemental Information.

### RNA extraction and analysis

RNA were extracted and analyzed by Northern blotting or real-time quantitative RT-PCR, mostly as previously described (Gachon et al., 2006). 5 μg of total RNA from four mice were used for northern blot experiments. As templates, we used pBluescript-KS$^+$ vectors containing RT-PCR products of the indicated gene (details of the probes can be found in Supplemental Information). In each case, membranes were stained with methylene blue before hybridization and stained 18S RNA is shown as a loading reference.

For the quantification of the spliced form of *Xbp1* by real-time RT-PCR, the experiments are realized as previously described (Lipson et al., 2006). 0.5 μg of liver whole cell RNA were reverse-transcribed using random hexamers and Superscript reverse transcriptase (Gibco, San Diego). The cDNA equivalent to 20 ng of total RNA was PCR-amplified in a MyiQ real-time PCR detection system (Bio-Rad). Primers sequences used for all the other experiments are given in Supplemental Information. In each case, average and standard deviation from at least three independent experiments are given using *Gapdh* mRNA as control.

**Protein extraction and analysis**

Nuclear proteins are extracted as described (Gachon et al., 2006). 25 μg of extracts were used for Western-blotting. For total extracts, liver were homogenized in lysis buffer containing 20 mM HEPES (pH 7.6), 100 mM KCl, 0.1 mM EDTA, 1 mM NaF, 1 mM sodium orthovanadate, 1% Triton X-100, 0.5% Nonidet P-40, 0.15 mM Spermine, 0.5 mM Spermidine, 1 mM DTT and protease inhibitors cocktail. 60 μg of extracts were used for Western-blotting. After migration, proteins were transferred to PVDF membranes and Western blotting realized according to standard procedures. References of the antibodies are given in Supplemental Information.

**Serum chemistry analysis**

Blood samples were collected at ZT0 after one complete night (12 hours) of fasting. Sera were collected

after centrifugation during 10 minutes at 3000 rpm at room temperature and subsequently kept at -80°C until analysis. Triglyceride, total cholesterol and glucose were measured using the LabAssay corresponding kit (Wako Chemicals), and free fatty acids were measured using the Half micro test (Roche Diagnostics) according to manufacturer instructions.

**Extraction and measure of concentrations of lipids in mouse liver**

Lipids were extracted by the Folch method. Briefly, 150 mg of liver were homogenized with 3 ml of a chloroform/methanol (2/1) solution and the mixture was agitated at room temperature for 2 hours. The homogenate was centrifuged to recover the liquid phase and the solvent was washed with 0.2 volume of a 0.9% NaCl solution. After few seconds of agitation with a vortex, the mixture was centrifuged at low speed to separate the two phases. The lower chloroform phase containing lipids was recovered and evaporated under vacuum in a rotary evaporator. The pellet was resuspended in 50 µl chloroform; and triglycerides and cholesterol concentrations were measured as described for serum.

## Acknowledgements

We thank Angélique Bruyer, Mayssa Chawaf, Vuthy Ea and Géraldine Bello for technical assistance, and Patrick Atger for his expert preparation of the artwork. We are very grateful to Xavier Bonnefont and Isabelle Bur for *Cry1*/*Cry2* knockout mice and for critical reading of the manuscript. We also want to thank Joseph Takahashi for liver mRNA from *ClockΔ19* mice, and David Weaver and Dmitri Firsov to give us access to *Clock* knockout mice. *Ire1α* cDNA was kindly provided by David Ron. We want to thank Ueli Schibler, Vjekoslav Dulic and Rosemary Kiernan for critical reading of this manuscript and John Hogenesch for sharing unpublished data with us. This research was supported by Inserm through the Avenir program,

by the "*Fondation pour la recherche Médicale*" and by the "*Association pour la Recherche sur le Cancer"*. G.C. is supported by a grant from Inserm and region Languedoc Roussillon. M. Le C. is supported by Inserm.

## References

Blander, G., and Guarente, L. (2004). The Sir2 family of protein deacetylases. Annu Rev Biochem. 73, 417-435.

Bobrovnikova-Marjon, E., Hatzivassiliou, G., Grigoriadou, C., Romero, M., Cavener, D.R., Thompson, C.B., and Diehl, J.A. (2008). PERK-dependent regulation of lipogenesis during mouse mammary gland development and adipocyte differentiation. Proc Natl Acad Sci U S A. 105, 16314-16319.

Bur, I.M., Cohen-Solal, A.M., Carmignac, D., Abecassis, P.-Y., Chauvet, N., Martin, A.O., van der Horst, G.T.J., Robinson, I.C.A.F., Maurel, P., Mollard, P., and Bonnefont, X. (2009). The Circadian Clock Components CRY1 and CRY2 Are Necessary to Sustain Sex Dimorphism in Mouse Liver Metabolism. J. Biol. Chem. 284, 9066-9073.

Calfon, M., Zeng, H., Urano, F., Till, J.H., Hubbard, S.R., Harding, H.P., Clark, S.G., and Ron, D. (2002). IRE1 couples endoplasmic reticulum load to secretory capacity by processing the XBP-1 mRNA. Nature 415, 92-96.

Chedid, A., and Nair, V. (1972). Diurnal Rhythm in Endoplasmic Reticulum of Rat Liver: Electron Microscopic Study. Science 175, 176-179.

Chen, Z., Odstrcil, E.A., Tu, B.P., and McKnight, S.L. (2007). Restriction of DNA Replication to the Reductive Phase of the Metabolic Cycle Protects Genome Integrity. Science 316, 1916-1919.

Cherrington, A.D., Stevenson, R.W., Steiner, K.E., Davis, M.A., Myers, S.R., Adkins, B.A., Abumrad, N.N., and Williams, P.E. (1987). Insulin, glucagon, and glucose as regulators of hepatic glucose uptake and production *in vivo*. Diabetes Metab Rev. 3, 307-332.

Colgan, S.M., Tang, D., Werstuck, G.H., and Austin, R.C. (2007). Endoplasmic reticulum stress causes the activation of sterol regulatory element binding protein-2. Int J Biochem Cell Biol. 39, 1843-1851.

Damiola, F., Le Minh, N., Preitner, N., Kornmann, B., Fleury-Olela, F., and Schibler, U. (2000). Restricted feeding uncouples circadian oscillators in peripheral tissues from the central pacemaker in the suprachiasmatic nucleus. Genes Dev. 14, 2950-2961.

De Man, J.C.H., Blok, A.P.R., and Beens, W. (1966). Relationship between glycogen and agranular endoplasmic reticulum in rat hepatic cells. J. Histochem. Cytochem. 14, 135-146.

DeBruyne, J.P., Noton, E., Lambert, C.M., Maywood, E.S., Weaver, D.R., and Reppert, S.M. (2006). A Clock Shock: Mouse CLOCK Is Not Required for Circadian Oscillator Function. Neuron 50, 465-477.

Espenshade, P.J., and Hughes, A.L. (2007). Regulation of Sterol Synthesis in Eukaryotes. Annu Rev Genet. 41, 401-427.

Feng, B., Yao, P.M., Li, Y., Devlin, C.M., Zhang, D., Harding, H.P., Sweeney, M., Rong, J.X., Kuriakose, G., Fisher, E.A., Marks, A.R., Ron, D., and Tabas, I. (2003). The endoplasmic reticulum is the site of cholesterol-induced cytotoxicity in macrophages. Nat Cell Biol 5, 781-792.

Flowers, M.T., Keller, M.P., Choi, Y., Lan, H., Kendziorski, C., Ntambi, J.M., and Attie, A.D. (2008). Liver gene expression analysis reveals endoplasmic reticulum stress and metabolic dysfunction in SCD1-deficient mice fed a very low-fat diet. Physiol. Genomics 33, 361-372.

Gachon, F. (2007). Physiological function of PARbZip circadian clock-controlled transcription factors. Ann Med. 39, 562 - 571.

Gachon, F., Fleury Olela, F., Schaad, O., Descombes, P., and Schibler, U. (2006). The circadian PAR-domain basic leucine zipper transcription factors DBP, TEF, and HLF modulate basal and inducible xenobiotic detoxification. Cell Metab. 4, 25-36.

Gachon, F., Fonjallaz, P., Damiola, F., Gos, P., Kodama, T., Zakany, J., Duboule, D., Petit, B., Tafti, M., and Schibler, U. (2004). The loss of circadian PAR bZip transcription factors results in epilepsy. Genes Dev. 18, 1397-1412.

Gallego, M., and Virshup, D.M. (2007). Post-translational modifications regulate the ticking of the circadian clock. Nat Rev Mol Cell Biol 8, 139-148.

Gill, A., Gao, N., and Lehrman, M.A. (2002). Rapid Activation of Glycogen Phosphorylase by the Endoplasmic Reticulum Unfolded Protein Response. J. Biol. Chem. 277, 44747-44753.

Gonzales, J., Gentile, C., Pfaffenbach, K., Wei, Y., Wang, D., and Pagliassotti, M. (2008). Chemical induction of the unfolded protein response in the liver increases glucose production and is activated during insulin-induced hypoglycaemia in rats. Diabetologia 51, 1920-1929.

Green, C.B., Takahashi, J.S., and Bass, J. (2008). The Meter of Metabolism. Cell 134, 728-742.

Hampton, R.Y. (2002). Proteolysis and sterol regulation. Annu Rev Cell Dev Biol. 18, 345-378.

Han, D., Lerner, A.G., Vande Walle, L., Upton, J.-P., Xu, W., Hagen, A., Backes, B.J., Oakes, S.A., and Papa, F.R. (2009). IRE1α Kinase Activation Modes Control Alternate Endoribonuclease Outputs to Determine Divergent Cell Fates. Cell 138, 562-575.

Hollien, J., Lin, J.H., Li, H., Stevens, N., Walter, P., and Weissman, J.S. (2009). Regulated Ire1-dependent decay of messenger RNAs in mammalian cells. J. Cell Biol. 186, 323-331.

Hollien, J., and Weissman, J.S. (2006). Decay of Endoplasmic Reticulum-Localized mRNAs During the Unfolded Protein Response. Science 313, 104-107.

Horton, J.D., Shah, N.A., Warrington, J.A., Anderson, N.N., Park, S.W., Brown, M.S., and Goldstein, J.L. (2003). Combined analysis of oligonucleotide microarray data from transgenic and knockout mice identifies direct SREBP target genes. Proc Natl Acad Sci U S A. 100, 12027-12032.

Huang, P., Ceccatelli, S., and Rannug, A. (2002). A study on diurnal mRNA expression of CYP1A1, AHR, ARNT, and PER2 in rat pituitary and liver. Environ. Toxicol. Pharmacol. 11, 119-126.

Hughes, M.E., DiTacchio, L., Hayes, K.R., Vollmers, C., Pulivarthy, S., Baggs, J.E., Panda, S., and Hogenesch, J.B. (2009). Harmonics of Circadian Gene Transcription in Mammals. PLoS Genet 5, e1000442.

Kato, H., Sakaki, K., and Mihara, K. (2006). Ubiquitin-proteasome-dependent degradation of mammalian ER stearoyl-CoA desaturase. J Cell Sci 119, 2342-2353.

Keller, R.K., Boon, D.Y., and Crum, F.C. (2002). N-Acetylglucosamine-1-phosphate transferase from hen oviduct: solubilization, characterization, and inhibition by tunicamycin. Biochemistry 18, 3946-3952.

Kim, S.Y., Jun, H.S., Mead, P.A., Mansfield, B.C., and Chou, J.Y. (2008). Neutrophil stress and apoptosis underlie myeloid dysfunction in glycogen storage disease type Ib. Blood 111, 5704-5711.

Kimball, S.R., and Jefferson, L.S. (1994). Mechanisms of translational control in liver and skeletal muscle. Biochimie 76, 729-736.

King, D.P., Zhao, Y., Sangoram, A.M., Wilsbacher, L.D., Tanaka, M., Antoch, M.P., Steeves, T.D.L., Vitaterna, M.H., Kornhauser, J.M., Lowrey, P.L., Turek, F.W., and Takahashi, J.S. (1997). Positional Cloning of the Mouse Circadian Clock Gene. Cell 89, 641-653.

Le Martelot, G., Claudel, T., Gatfield, D., Schaad, O., Kornmann, B., Sasso, G.L., Moschetta, A., and Schibler, U. (2009). REV-ERBα Participates in Circadian SREBP Signaling and Bile Acid Homeostasis. PLoS Biol 7, e1000181.

Lee, A.-H., and Glimcher, L. (2009). Intersection of the unfolded protein response and hepatic lipid metabolism. Cell Mol Life Sci.

Lee, A.-H., Scapa, E.F., Cohen, D.E., and Glimcher, L.H. (2008). Regulation of Hepatic Lipogenesis by the Transcription Factor XBP1. Science 320, 1492-1496.

Lee, J.N., and Ye, J. (2004). Proteolytic Activation of Sterol Regulatory Element-binding Protein Induced by Cellular Stress through Depletion of Insig-1. J. Biol. Chem. 279, 45257-45265.

Lee, K., Tirasophon, W., Shen, X., Michalak, M., Prywes, R., Okada, T., Yoshida, H., Mori, K., and Kaufman, R.J. (2002). IRE1-mediated unconventional mRNA splicing and S2P-mediated ATF6 cleavage merge to regulate XBP1 in signaling the unfolded protein response. Genes Dev. 16, 452-466.

Lindenmeyer, M.T., Rastaldi, M.P., Ikehata, M., Neusser, M.A., Kretzler, M., Cohen, C.D., and Schlondorff, D. (2008). Proteinuria and Hyperglycemia Induce Endoplasmic Reticulum Stress. J Am Soc Nephrol 19, 2225-2236.

Lipson, K.L., Fonseca, S.G., Ishigaki, S., Nguyen, L.X., Foss, E., Bortell, R., Rossini, A.A., and Urano, F. (2006). Regulation of insulin biosynthesis in pancreatic beta cells by an endoplasmic reticulum-resident protein kinase IRE1. Cell Metab. 4, 245-254.

Little, J.L., Wheeler, F.B., Fels, D.R., Koumenis, C., and Kridel, S.J. (2007). Inhibition of Fatty Acid Synthase Induces Endoplasmic Reticulum Stress in Tumor Cells. Cancer Res 67, 1262-1269.

Marciniak, S.J., and Ron, D. (2006). Endoplasmic Reticulum Stress Signaling in Disease. Physiol. Rev. 86, 1133-1149.

Meusser, B., Hirsch, C., Jarosch, E., and Sommer, T. (2005). ERAD: the long road to destruction. Nat Cell Biol 7, 766-772.

Miller, B.H., McDearmon, E.L., Panda, S., Hayes, K.R., Zhang, J., Andrews, J.L., Antoch, M.P., Walker, J.R., Esser, K.A., Hogenesch, J.B., and Takahashi, J.S. (2007). Circadian and CLOCK-controlled regulation of the mouse transcriptome and cell proliferation. Proc Natl Acad Sci U S A. 104, 3342-3347.

Mio, T., Yabe, T., Arisawa, M., and Yamada-Okabe, H. (1998). The Eukaryotic UDP-N-Acetylglucosamine Pyrophosphorylases. Gene cloning, protein expression, and catalytic mechanism. J. Biol. Chem. 273, 14392-14397.

Morgan, C.R., and Jersild, R.A.J. (1970). Alterations in the morphology of rat liver cells influenced by insulin. Anat Rec. 166, 575-585.

Ota, T., Gayet, C., and Ginsberg, H.N. (2008). Inhibition of apolipoprotein B100 secretion by lipid-induced hepatic endoplasmic reticulum stress in rodents. J Clin Invest. 118, 316-332.

Oyadomari, S., Harding, H.P., Zhang, Y., Oyadomari, M., and Ron, D. (2008). Dephosphorylation of Translation Initiation Factor 2α Enhances Glucose Tolerance and Attenuates Hepatosteatosis in Mice. Cell Metab. 7, 520-532.

Ozcan, U., Cao, Q., Yilmaz, E., Lee, A.-H., Iwakoshi, N.N., Ozdelen, E., Tuncman, G., Gorgun, C., Glimcher, L.H., and Hotamisligil, G.S. (2004). Endoplasmic Reticulum Stress Links Obesity, Insulin Action, and Type 2 Diabetes. Science 306, 457-461.

Ozcan, U., Yilmaz, E., Ozcan, L., Furuhashi, M., Vaillancourt, E., Smith, R.O., Gorgun, C.Z., and Hotamisligil, G.S. (2006). Chemical Chaperones Reduce ER Stress and Restore Glucose Homeostasis in a Mouse Model of Type 2 Diabetes. Science 313, 1137-1140.

Prasai, M.J., George, J.T., and Scott, E.M. (2008). Molecular clocks, type 2 diabetes and cardiovascular disease. Diab Vasc Dis Res. 5, 89-95.

Qu, X., Metz, R.P., Porter, W.W., Cassone, V.M., and Earnest, D.J. (2007). Disruption of Clock Gene Expression Alters Responses of the Aryl Hydrocarbon Receptor Signaling Pathway in the Mouse Mammary Gland. Mol Pharmacol 72, 1349-1358.

Ramsey, K.M., Yoshino, J., Brace, C.S., Abrassart, D., Kobayashi, Y., Marcheva, B., Hong, H.-K., Chong, J.L., Buhr, E.D., Lee, C., Takahashi, J.S., Imai, S.-i., and Bass, J. (2009). Circadian Clock Feedback Cycle Through NAMPT-Mediated $NAD^+$ Biosynthesis. Science 324, 651-654.

Ron, D., and Walter, P. (2007). Signal integration in the endoplasmic reticulum unfolded protein response. Nat Rev Mol Cell Biol 8, 519-529.

Rutkowski, D.T., Wu, J., Back, S.-H., Callaghan, M.U., Ferris, S.P., Iqbal, J., Clark, R., Miao, H., Hassler, J.R., Fornek, J., Katze, M.G., Hussain, M.M., Song, B., Swathirajan, J., Wang, J., Yau, G.D.Y., and Kaufman, R.J. (2008). UPR Pathways Combine to Prevent Hepatic Steatosis Caused by ER Stress-Mediated Suppression of Transcriptional Master Regulators. Dev Cell 15, 829-840.

Scheer, F.A.J.L., Hilton, M.F., Mantzoros, C.S., and Shea, S.A. (2009). Adverse metabolic and cardiovascular consequences of circadian misalignment. Proc Natl Acad Sci U S A. 106, 4453-4458.

Schröder, M., and Kaufman, R.J. (2005). The mammalian unfolded protein response. Annu Rev Biochem. 74, 739-789.

Sesma, J.I., Esther, C.R., Jr., Kreda, S.M., Jones, L., O'Neal, W., Nishihara, S., Nicholas, R.A., and Lazarowski, E.R. (2009). Endoplasmic Reticulum/Golgi Nucleotide Sugar Transporters Contribute to the Cellular Release of UDP-sugar Signaling Molecules. J. Biol. Chem. 284, 12572-12583.

Sriburi, R., Jackowski, S., Mori, K., and Brewer, J.W. (2004). XBP1: a link between the unfolded protein response, lipid biosynthesis, and biogenesis of the endoplasmic reticulum. J. Cell Biol. 167, 35-41.

Szczesna-Skorupa, E., Chen, C.-D., Liu, H., and Kemper, B. (2004). Gene Expression Changes Associated with the Endoplasmic Reticulum Stress Response Induced by Microsomal Cytochrome P450 Overproduction. J Biol Chem. 279, 13953-13961.

Thuerauf, D.J., Morrison, L.E., Hoover, H., and Glembotski, C.C. (2002). Coordination of ATF6-mediated Transcription and ATF6 Degradation by a Domain That Is Shared with the Viral Transcription Factor, VP16. J. Biol. Chem. 277, 20734-20739.

Tirasophon, W., Lee, K., Callaghan, B., Welihinda, A., and Kaufman, R.J. (2000). The endoribonuclease activity of mammalian IRE1 autoregulates its mRNA and is required for the unfolded protein response. Genes Dev. 14, 2725-2736.

Tu, B.P., Kudlicki, A., Rowicka, M., and McKnight, S.L. (2005). Logic of the Yeast Metabolic Cycle: Temporal Compartmentalization of Cellular Processes. Science 310, 1152-1158.

Tu, B.P., Mohler, R.E., Liu, J.C., Dombek, K.M., Young, E.T., Synovec, R.E., and McKnight, S.L. (2007). Cyclic changes in metabolic state during the life of a yeast cell. Proc Natl Acad Sci U S A. 104, 16886-16891.

Turek, F.W., Joshu, C., Kohsaka, A., Lin, E., Ivanova, G., McDearmon, E., Laposky, A., Losee-Olson, S., Easton, A., Jensen, D.R., Eckel, R.H., Takahashi, J.S., and Bass, J. (2005). Obesity and Metabolic Syndrome in Circadian Clock Mutant Mice. Science 308, 1043-1045.

Uyeda, K., and Repa, J.J. (2006). Carbohydrate response element binding protein, ChREBP, a transcription factor coupling hepatic glucose utilization and lipid synthesis. Cell Metab. 4, 107-110.

van der Horst, G.T.J., Muijtjens, M., Kobayashi, K., Takano, R., Kanno, S.-i., Takao, M., de Wit, J., Verkerk, A., Eker, A.P.M., van Leenen, D., Buijs, R., Bootsma, D., Hoeijmakers, J.H.J., and Yasui, A. (1999). Mammalian Cry1 and Cry2 are essential for maintenance of circadian rhythms. Nature 398, 627-630.

Vitaterna, M.H., King, D.P., Chang, A.M., Kornhauser, J.M., Lowrey, P.L., McDonald, J.D., Dove, W.F., Pinto, L.H., Turek, F.W., and Takahashi, J.S. (1994). Mutagenesis and mapping of a mouse gene, *Clock*, essential for circadian behavior. Science 264, 719-725.

Volpe, J.J., and Goldberg, R.I. (1983). Effect of tunicamycin on 3-hydroxy-3-methylglutaryl coenzyme A reductase in C-6 glial cells. J Biol Chem 258, 9220-9226.

Wang, H., Kouri, G., and Wollheim, C.B. (2005). ER stress and SREBP-1 activation are implicated in β-cell glucolipotoxicity. J Cell Sci 118, 3905-3915.

Wang, X.Z., Lawson, B., Brewer, J.W., Zinszner, H., Sanjay, A., Mi, L.J., Boorstein, R., Kreibich, G., Hendershot, L.M., and Ron, D. (1996). Signals from the stressed endoplasmic reticulum induce C/EBP-homologous protein (CHOP/GADD153). Mol. Cell. Biol. 16, 4273-4280.

Yoshida, H., Matsui, T., Hosokawa, N., Kaufman, R.J., Nagata, K., and Mori, K. (2003). A Time-Dependent Phase Shift in the Mammalian Unfolded Protein Response. Dev Cell 4, 265-271.

Yoshida, H., Matsui, T., Yamamoto, A., Okada, T., and Mori, K. (2001). XBP1 mRNA Is Induced by ATF6 and Spliced by IRE1 in Response to ER Stress to Produce a Highly Active Transcription Factor. Cell 107, 881-891.

## Figure legends

**Figure 1: Time-dependent induction of the Unfolded Protein Response (UPR) by Tunicamycin in mouse liver.**

Tunicamycin or DMSO was injected i.p. every 4 hours during 24 hours and mice were sacrificed 4 hours after the injection. The *Zeitgeber* times (ZT) at which the animals were sacrificed are indicated on the figure. For all the panels, continue and dashed lines represent DMSO and Tunicamycin treatment, respectively. Data are Mean ± SEM obtained from two independent experiments.

A. Temporal activation of the representative actors of the three UPR pathways. Western blots were realized on total (ATF6α) or nuclear liver extracts. $U2AF^{65}$ was used as a loading control.

B. Temporal real-time RT-PCR profile of spliced and total *Xbp1* mRNA in mouse liver after Tunicamycin injection.

C. Temporal real-time RT-PCR profile of the UPR regulated genes *Bip* and *Chop* mRNA in mouse liver after Tunicamycin injection.

D. Temporal real-time RT-PCR profile of the xenobiotic induced gene *Cyp2b10* mRNA in mouse liver after Tunicamycin injection.

E. Mean ± SEM serum and liver triglycerides concentrations after Tunicamycin injection. Black and grey boxes represent DMSO and Tunicamycin treatment, respectively. Student's *t* test p values are given on the figure.

F. Liver temporal expression after Tunicamycin injection of enzymes involved in lipid metabolism that are sensitive (HMGCR and SCD1) or insensitive (FASN) to ER-associated degradation. Western blots were realized on total liver extracts and L28 ribosomal protein was used as a loading control.

**Figure 2: Basal 12 hours period rhythmic activation of the IRE1α pathway in mouse liver.**

A. Temporal expression of mRNA from UPR regulated genes in mouse liver by Northern blotting. The membranes were stained with methylene blue before hybridization, and stained 18S rRNA is shown as a loading reference.

B. Temporal phosphorylation of IRE1α at $Ser^{724}$ and expression of the total protein during two 24-hours cycles. L28 ribosomal protein was used as a loading control.

C. Temporal expression of *Ire1α* mRNA in mouse liver by Northern blotting.

D. Temporal profile of *Xbp1* mRNA processing in mouse liver as monitored by real-time RT-PCR. RNA from four mice are used for each time-point and the data are double-plotted. Data for total *Xbp1* mRNA are given on Figure S3A.

E. Temporal accumulation of XBP1 protein in liver nuclei during two 24-hours cycles. PER1 accumulation is shown as a control for diurnal synchronization of the animals and $U2AF^{65}$ as a loading control.

The *Zeitgeber* times (ZT) in hours at which the animals were sacrificed are indicated on the top of each figures.

**Figure 3: 12-hours period rhythmic activation of the IRE1α pathway is maintained uder constant conditions.**

A. Temporal activation of the IRE1α pathway during 48 hours in constant darkness.

B. Temporal activation of the IRE1α pathway during starvation.

For panels A and B, sub-panels represent: a. Temporal phosphorylation of IRE1α at $Ser^{724}$ and expression of the total protein. L28 ribosomal protein was used as a loading control. b. Temporal profile of *Xbp1* mRNA processing in mouse liver as monitored by real-time RT-PCR. RNA from two mice are used for each time-point. Total *Xbp1* mRNA expressions are given on Figure S3B and S3C, respectively. c. Temporal accumulation of XBP1 protein in liver nuclei. PER1 accumulation is given as a control for circadian or

diurnal synchronization of the animals and U2AF$^{65}$ as a loading control.

The circadian (CT) or *Zeitgeber* (ZT) times at which the animals were sacrificed are indicated on the top of the figures.

**Figure 4: Influence of the circadian clock on 12-hours period rhythmic activation of the IRE1α pathway in the liver.**

A. Temporal accumulation of nuclear XBP1 protein (upper panel) and Northern blotting analysis of the expression of the UPR regulated genes *Bip*, *Hrd1* and *Dnajb9* mRNA (lower panel) in liver from Wild-type (H++/D++/T++) and PARbZip ko (H--/D--/T--) mice.

B. Temporal activation of the IRE1α pathway in *Cry1*/*Cry2* ko mice. a. Temporal phosphorylation of IRE1α at Ser$^{724}$ and expression of the total protein during two 24-hours cycles. b. Temporal profile of *Xbp1* mRNA processing as monitored by real-time RT-PCR. RNA from two mice are used for each time-point and the data are double-plotted. Data for total *Xbp1* mRNA is given on Figure S3D. c. Temporal accumulation of XBP1 protein in liver nuclei. PER1 accumulation is given as a control for the arrhythmic behaviour of the molecular clock of these animals. d. Northern blotting analysis of the expression of the UPR regulated genes *Hrd1*, *Dnajb9* and *Chop* mRNA.

U2AF$^{65}$, L28 ribosomal protein and 18S rRNA are given as loading controls for Western blotting on nuclear and total proteins or Northern blotting, respectively. The *Zeitgeber* times (ZT) at which the animals were sacrificed are indicated on the top of the figure.

**Figure 5: Consequence of 12-hours period rhythmic activation of the IRE1α pathway on lipid metabolism.**

A. Liver temporal expression of enzymes involved in lipid metabolism that are sensitive (HMGCR and

SCD1) or insensitive (FASN) to ERAD in *Cry1*/*Cry2* ko mice. L28 ribosomal protein was used as a loading control.

B. Northern blot analysis of the mRNA expression for the SREBP target genes *Hmgcr*, *Scd1* and *Fasn*, in wild-type and *Cry1*/*Cry2* ko mice liver. 18S rRNA is shown as a loading reference.

C. Temporal accumulation of SREBP1 and SREBP2 in wild-type and *Cry1*/*Cry2* ko mice in liver nuclear extracts and of INSIG1 and INSIG2 on total extracts. $U2AF^{65}$ and L28 ribosomal protein are given as loading controls for nuclear and total proteins, respectively.

D. Northern blot analysis of the expression *Srebp1*, *Srebp2*, *Insig1* and *Insig2* mRNA in wild-type and *Cry1*/*Cry2* ko mice liver.

E. Mean ± SEM serum and liver triglycerides concentrations before and after TUDCA treatment. Black and grey boxes represent wild-type and *Cry1*/*Cry2* ko mice, respectively. Student's *t* test p values are given on the figure.

The *Zeitgeber* times (ZT) at which the animals were sacrificed are indicated on the figures.

**Figure 6: Temporal expression of UPR regulated genes and SREBP target genes in *ClockΔ19* mutant mice liver.**

Expression of the UPR regulated genes *Xbp1* (spliced and total mRNA), *Chop* and *Bip* (A) and of the SREBP regulated genes *Hmgcr*, *Fasn*, *Ldlr* and *Elovl6* (B) were measured by real-time RT-PCR on liver RNA from wild-type and *ClockΔ19* mutant mice kept in constant darkness. Data represent Mean ± SEM values obtained with RNA from two independent mice for each time-point.

**Figure 7: Model of the synchronization of the 12-hours period rhythmic activation of the IRE1α pathway by the liver circadian oscillator and feeding.**

Circadian clock regulated lipid metabolism induced 12-hours period rhythmic activation of IRE1α, leading to 12-hours period rhythmic expression of UPR regulated genes. As XBP1 has been shown to regulate lipid metabolism at transcriptional level (Lee et al., 2008) and post-translational level (this article), this activation of IRE1α could contribute to the lipid metabolism and then regulates its own activation. All this system could then constitute a 12-hours period oscillator synchronized by the circadian clock and feeding rhythms.

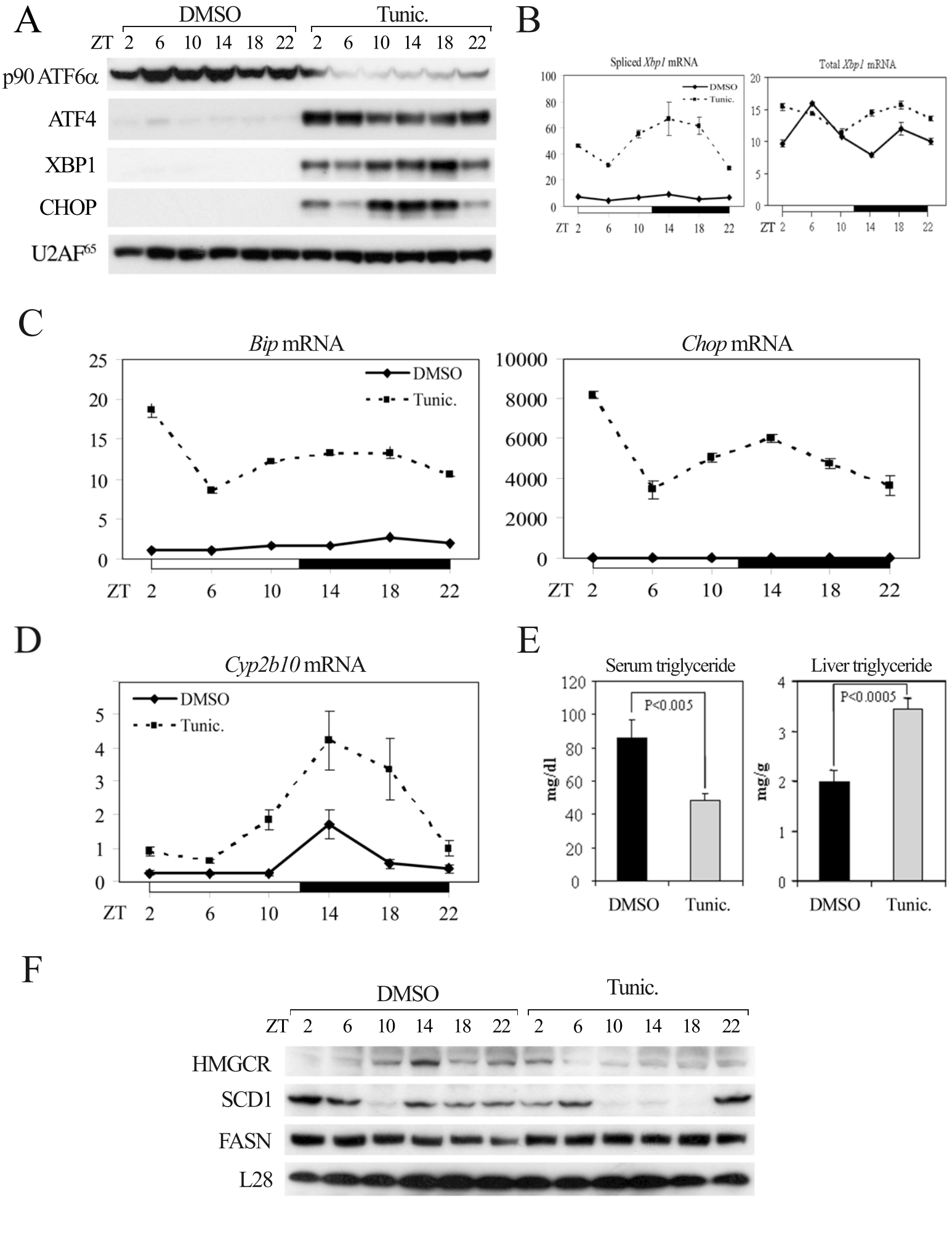
A
DMSO
Tunic.
ZT 2 6 10 14 18 22 2 6 10 14 18 22
p90 ATF6α
ATF4
XBP1
CHOP
U2AF65
B
Spliced Xbp1 mRNA
Total Xbp1 mRNA
DMSO
Tunic.
ZT 2 6 10 14 18 22
C
Bip mRNA
Chop mRNA
DMSO
Tunic.
ZT 2 6 10 14 18 22
D
Cyp2b10 mRNA
DMSO
Tunic.
ZT 2 6 10 14 18 22
E
Serum triglyceride
Liver triglyceride
P<0.005
P<0.0005
mg/dl
mg/g
DMSO
Tunic.
F
DMSO
Tunic.
ZT 2 6 10 14 18 22 2 6 10 14 18 22
HMGCR
SCD1
FASN
L28

Fig. 1

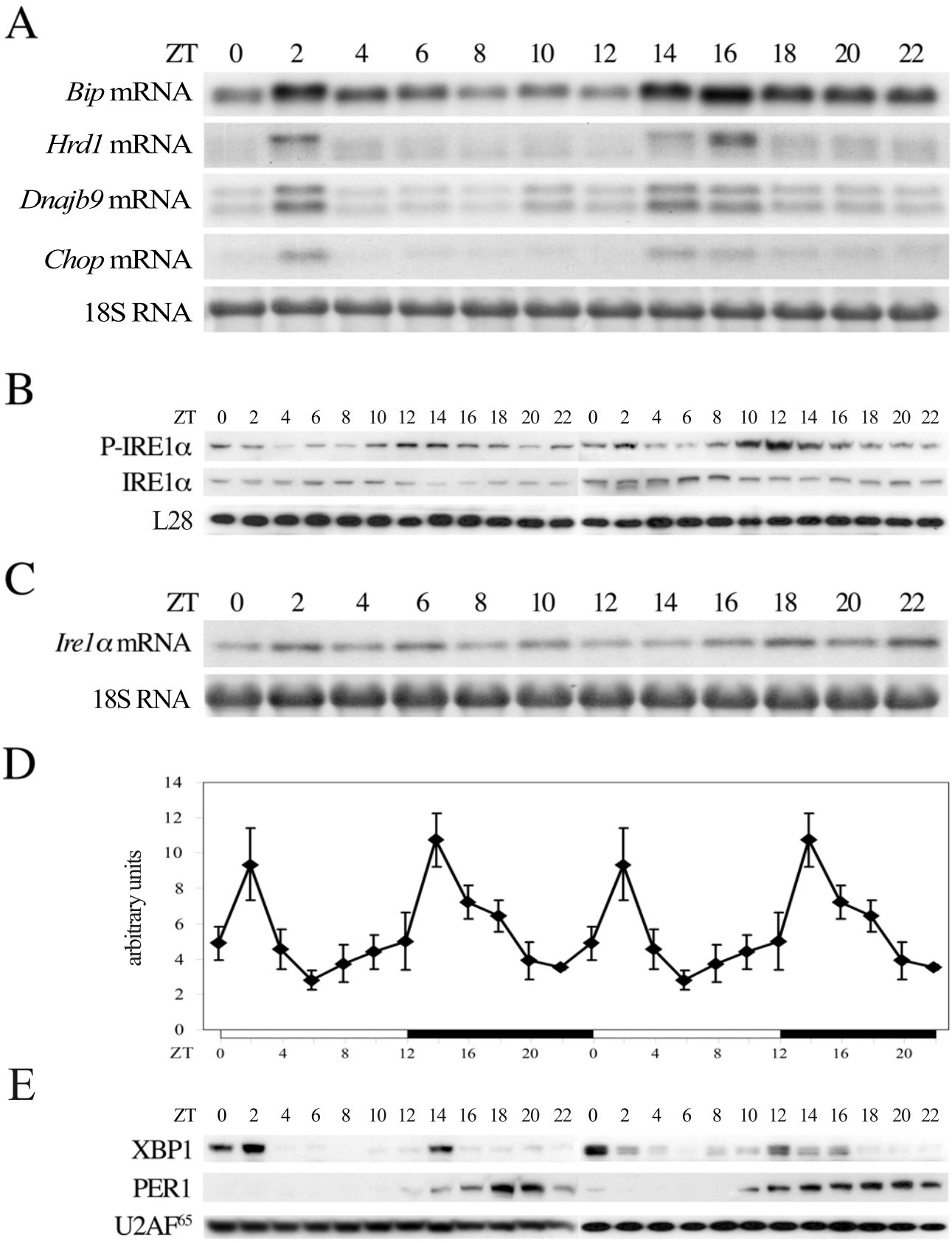
A
ZT 0 2 4 6 8 10 12 14 16 18 20 22
Bip mRNA
Hrd1 mRNA
Dnajb9 mRNA
Chop mRNA
18S RNA
B
ZT 0 2 4 6 8 10 12 14 16 18 20 22 0 2 4 6 8 10 12 14 16 18 20 22
P-IRE1α
IRE1α
L28
C
ZT 0 2 4 6 8 10 12 14 16 18 20 22
Ire1α mRNA
18S RNA
D
arbitrary units
0 2 4 6 8 10 12 14
ZT 0 4 8 12 16 20 0 4 8 12 16 20
E
ZT 0 2 4 6 8 10 12 14 16 18 20 22 0 2 4 6 8 10 12 14 16 18 20 22
XBP1
PER1
U2AF65

Fig. 2

A

a.

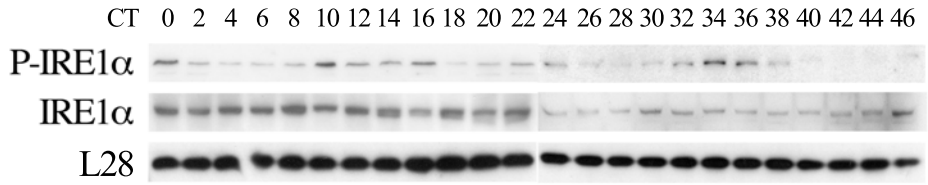


b.

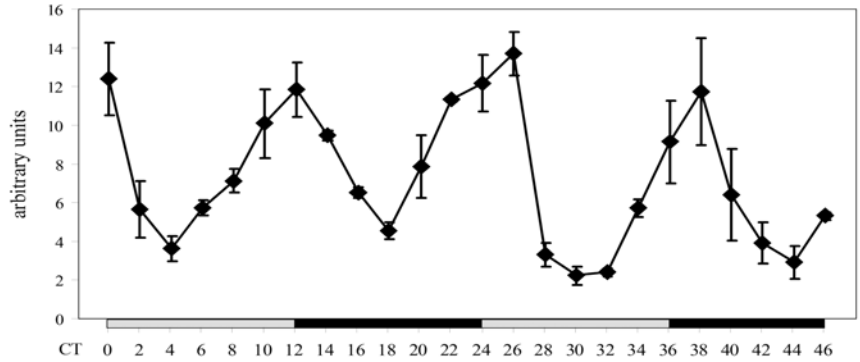


c.

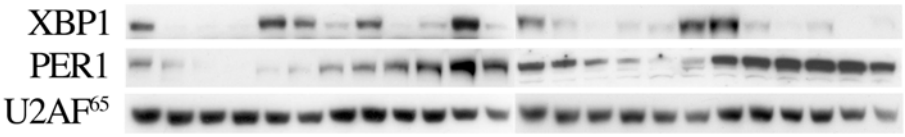


B

a.

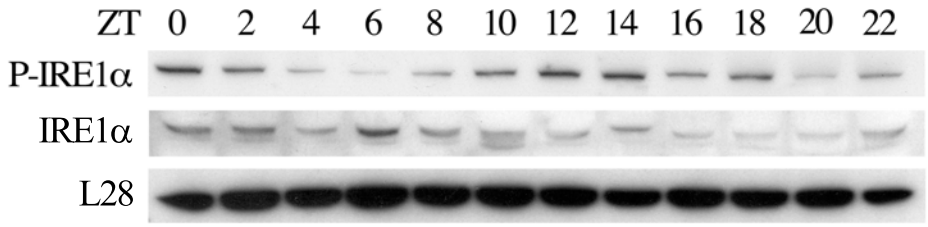


b.

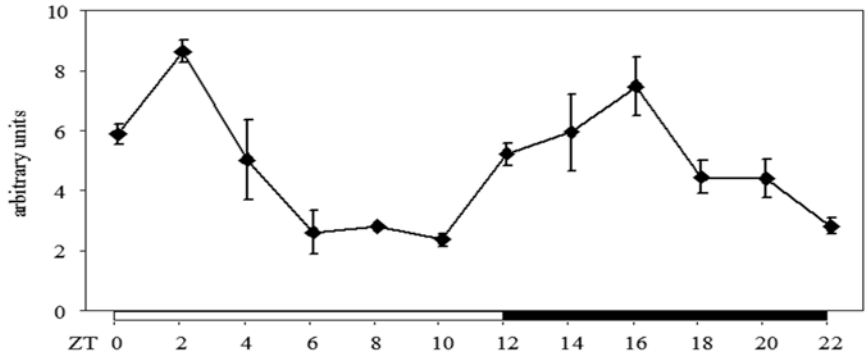


c.

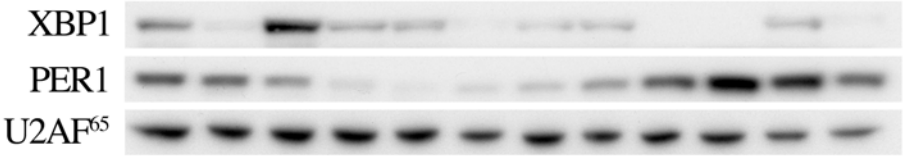


Fig. 3

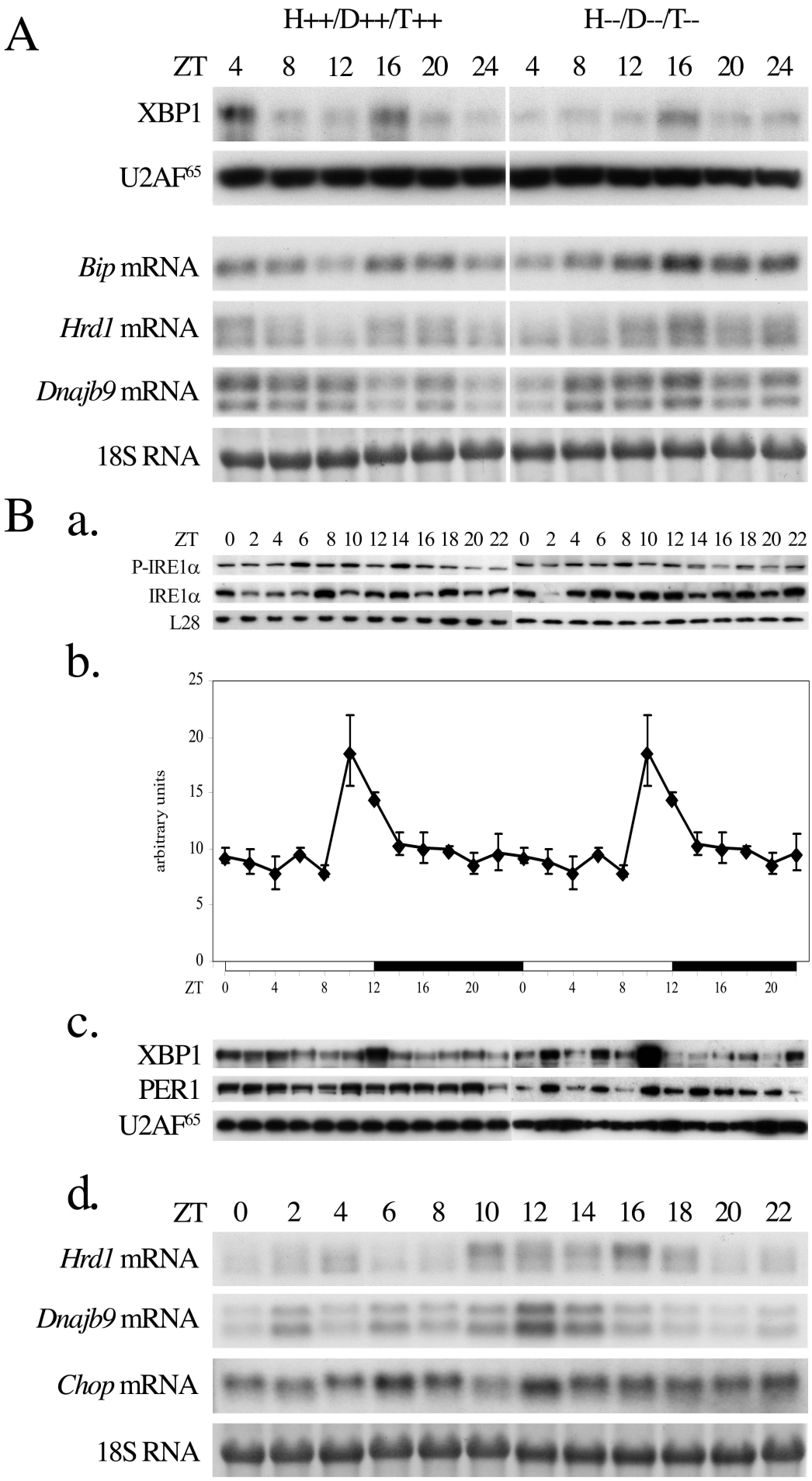
A
H++/D++/T++
H--/D--/T--
ZT 4 8 12 16 20 24 4 8 12 16 20 24
XBP1
U2AF65
Bip mRNA
Hrd1 mRNA
Dnajb9 mRNA
18S RNA
B a.
ZT 0 2 4 6 8 10 12 14 16 18 20 22 0 2 4 6 8 10 12 14 16 18 20 22
P-IRE1α
IRE1α
L28
b.
arbitrary units
25
20
15
10
5
0
ZT 0 4 8 12 16 20 0 4 8 12 16 20
c.
XBP1
PER1
U2AF65
d.
ZT 0 2 4 6 8 10 12 14 16 18 20 22
Hrd1 mRNA
Dnajb9 mRNA
Chop mRNA
18S RNA

Fig. 4

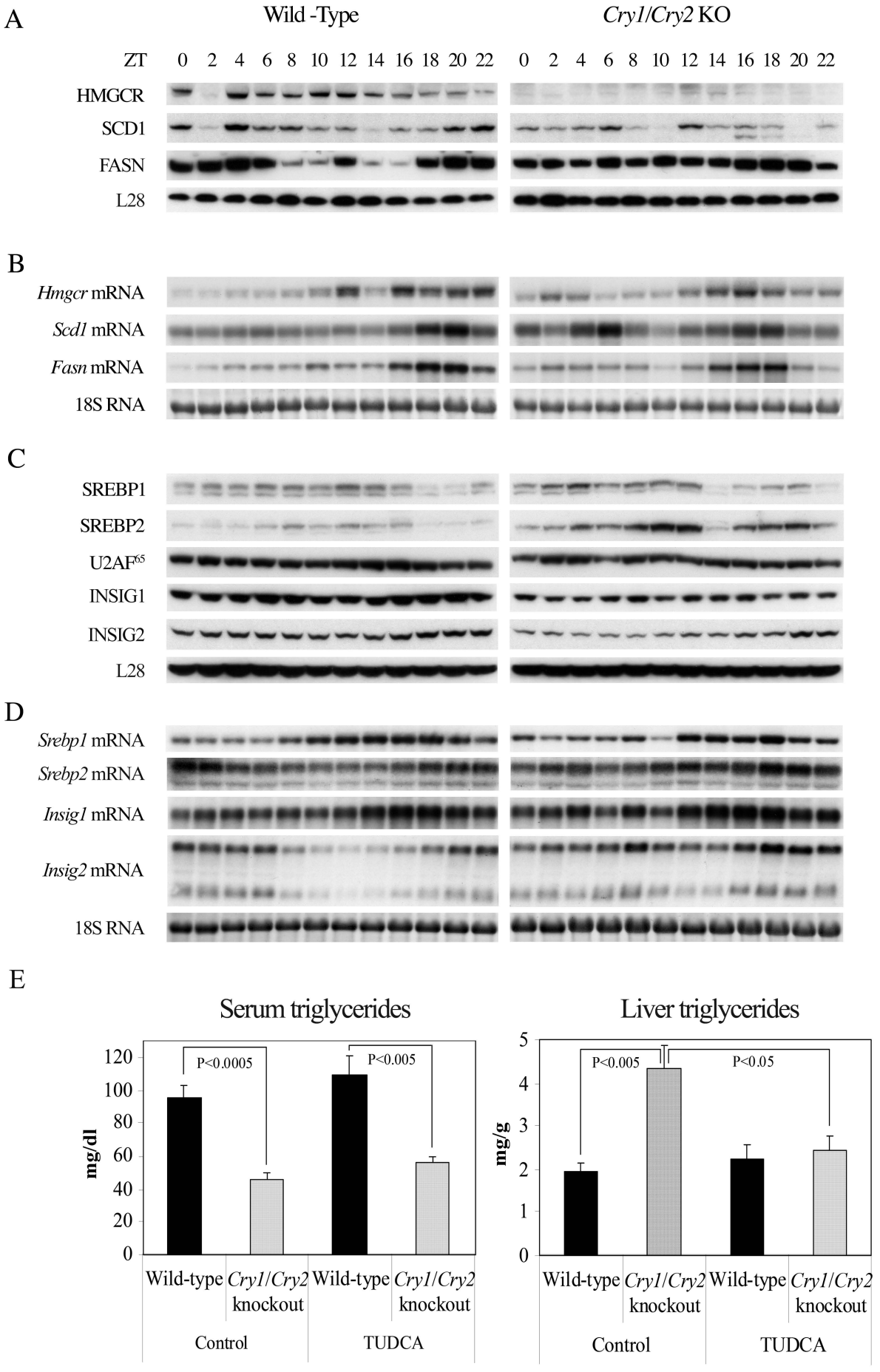
A
Wild -Type
Cry1/Cry2 KO
ZT 0 2 4 6 8 10 12 14 16 18 20 22 0 2 4 6 8 10 12 14 16 18 20 22
HMGCR
SCD1
FASN
L28
B
Hmgcr mRNA
Scd1 mRNA
Fasn mRNA
18S RNA
C
SREBP1
SREBP2
U2AF65
INSIG1
INSIG2
L28
D
Srebp1 mRNA
Srebp2 mRNA
Insig1 mRNA
Insig2 mRNA
18S RNA
E
Serum triglycerides
Liver triglycerides
mg/dl
mg/g
P<0.0005
P<0.005
P<0.005
P<0.05
Wild-type
Cry1/Cry2 knockout
Control
TUDCA

Fig. 5

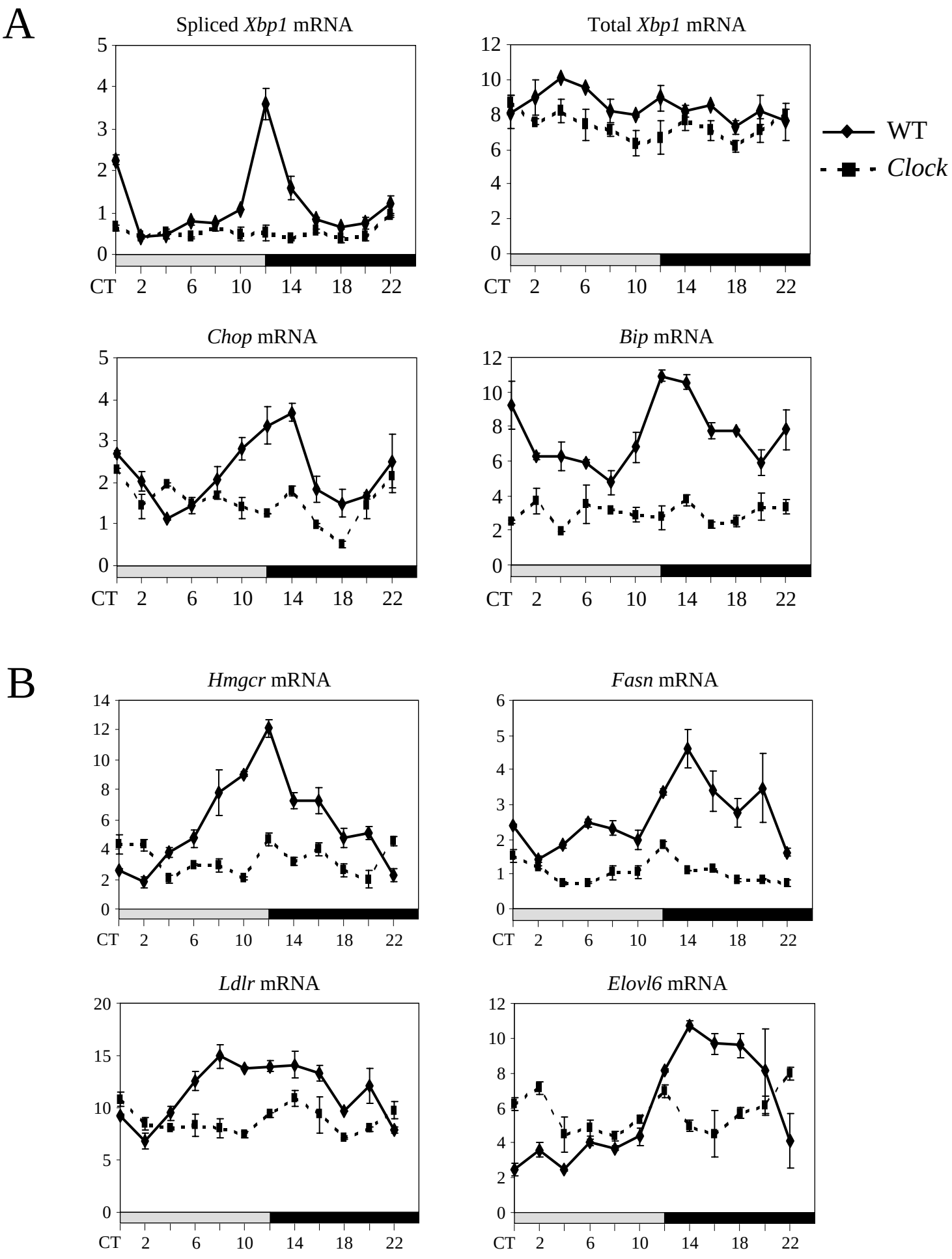
A
Spliced *Xbp1* mRNA
Total *Xbp1* mRNA
WT
*Clock*
*Chop* mRNA
*Bip* mRNA
B
*Hmgcr* mRNA
*Fasn* mRNA
*Ldlr* mRNA
*Elovl6* mRNA
CT 2 6 10 14 18 22

Fig. 6

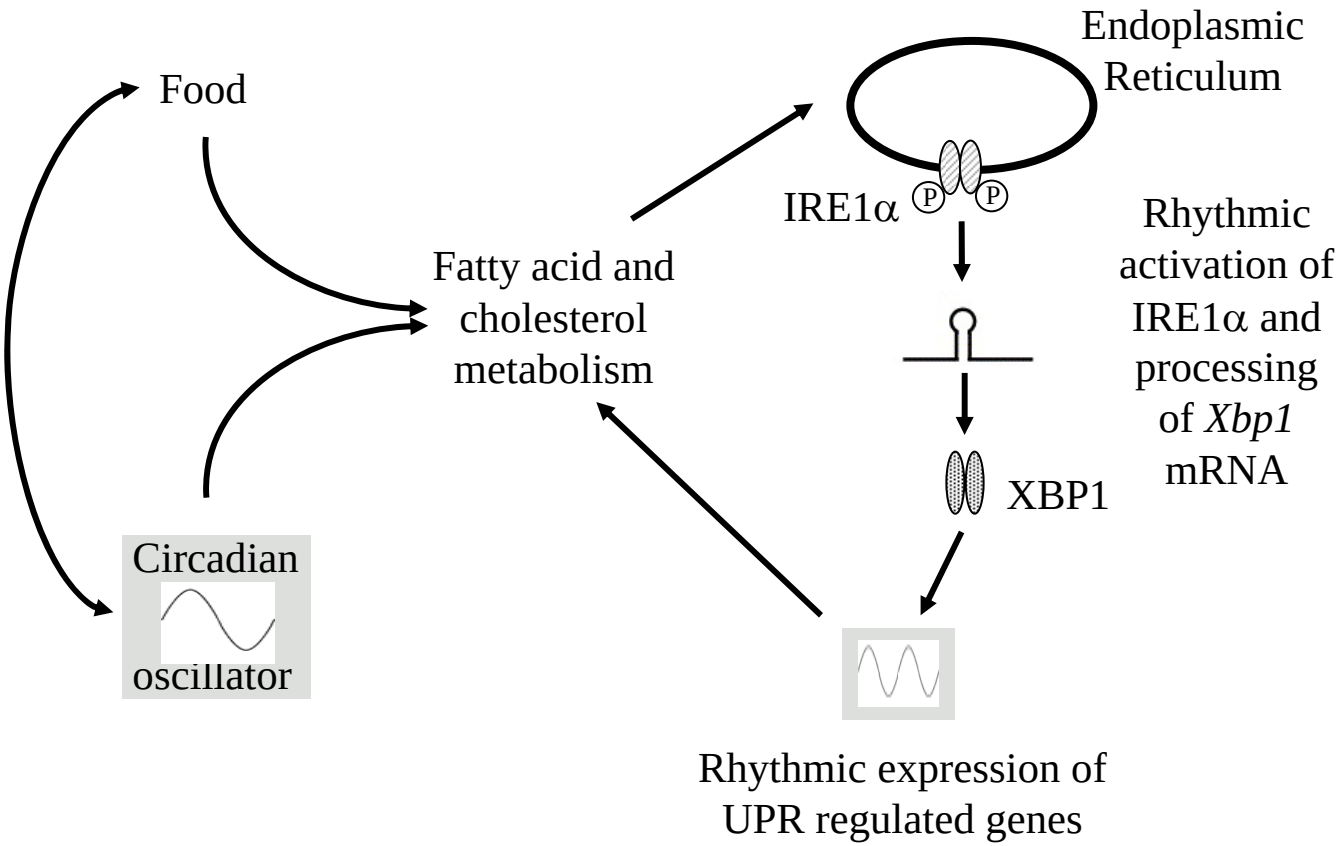
Endoplasmic
Reticulum
Food
IRE1α
P
P
Rhythmic
activation of
IRE1α and
processing
of *Xbp1*
mRNA
Fatty acid and
cholesterol
metabolism
XBP1
Circadian
oscillator
Rhythmic expression of
UPR regulated genes

Fig. 7

## Supplemental Information

**Figure S1: Influence of the time of Tunicamycin injection on the change in triglycerides and cholesterol concentrations**

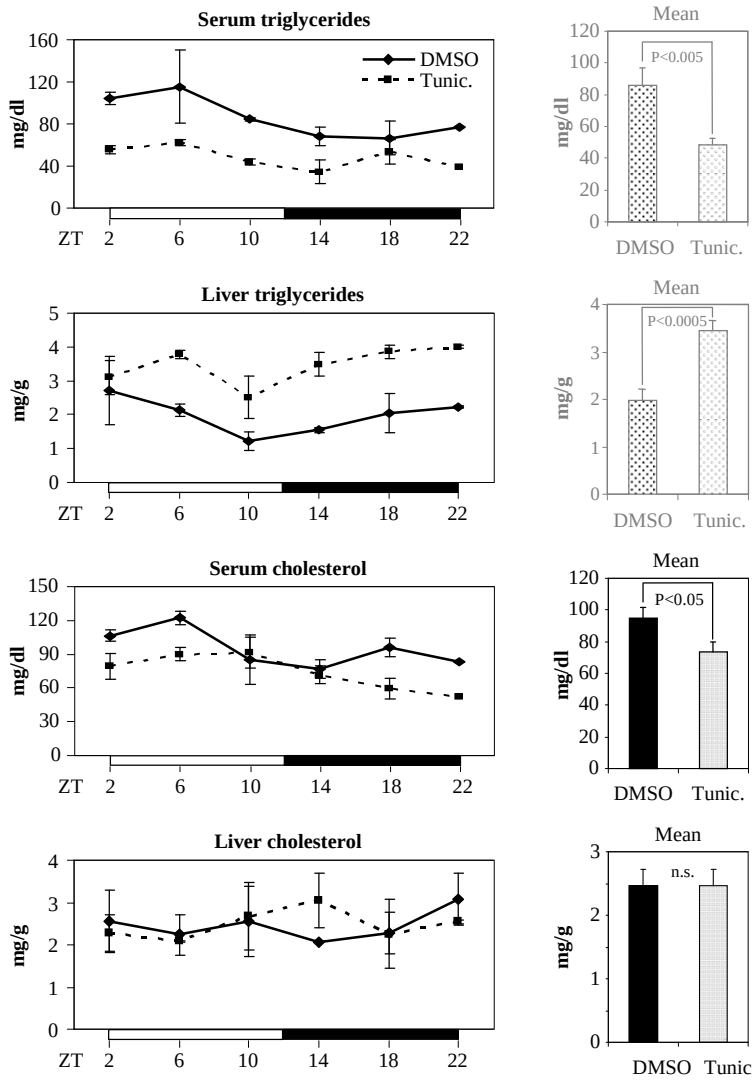


Left panels: Temporal concentrations (Mean ± SEM) of triglycerides and cholesterol in serum and liver of mice injected with Tunicamycin (1 mg/Kg) or equivalent volume of solvent (DMSO). The *Zeitgeber* times (ZT) at which the animals were sacrificed (4 hours after the injection) are indicated at the bottom of the figure. No significant time-dependent response to Tunicamycin was observed.

Right panels: Mean ± SEM of the values obtained at the different time points (Student's *t* test p values are given on the figure). The data obtained for triglycerides are also given on Figure 2. The results obtained are in accordance with those reported by Rutkowsi et al. (2008).

**Figure S2. Ultradian activation of the Unfolded Protein Response in mouse liver**

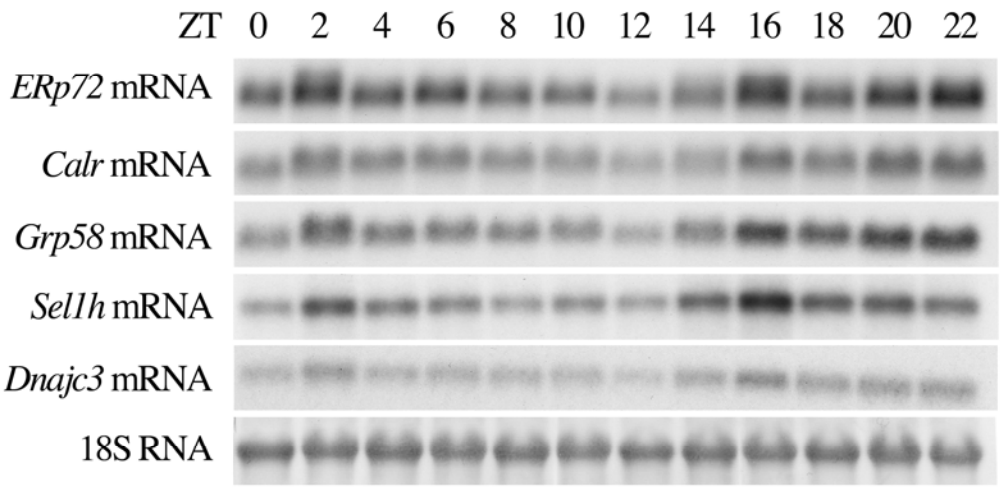


Temporal expression of mRNA from additional UPR regulated genes in mouse liver by Northern blotting. The rest of the UPR regulated genes can be found in Figure 1A. The *Zeitgeber* times (ZT) at which the animals were sacrificed are indicated on the top of the figure.

**Figure S3. Expression of total *Xbp1* mRNA in the liver of wild-type and *Cry1*/*Cry2* knockout mice under different conditions**

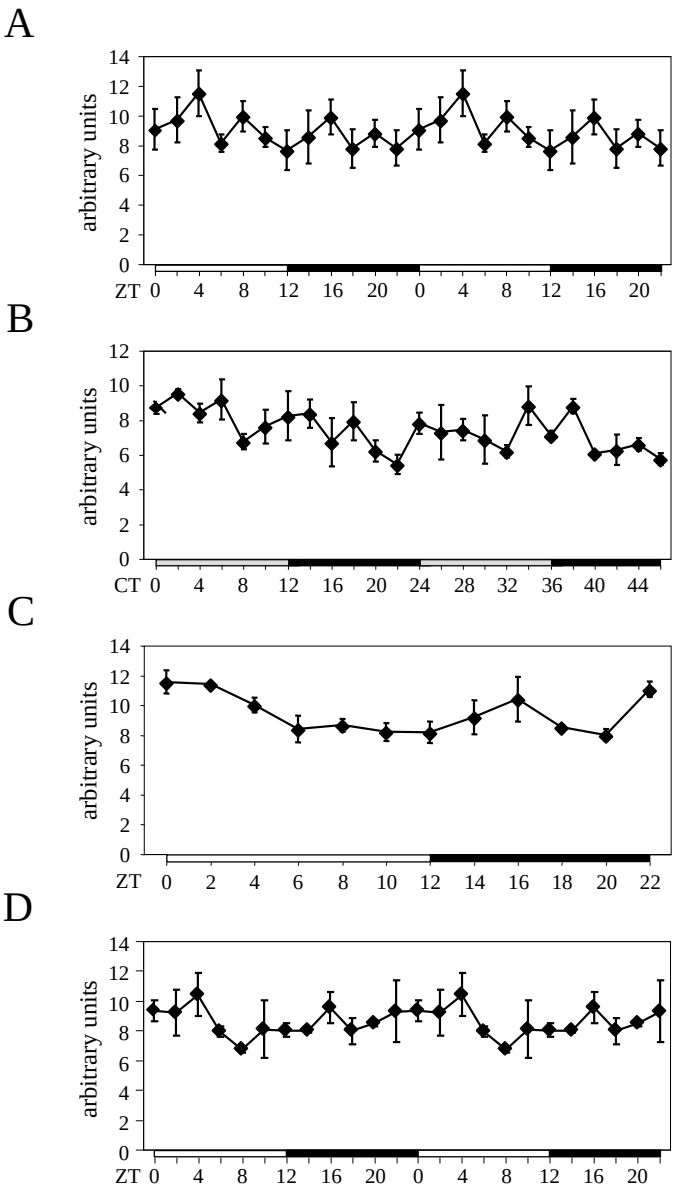


Temporal *Xbp1* total mRNA accumulation is in all cases measured by real-time RT-PCR.

A. Wild-type mice under the light-dark cycle. RNA from four mice are used for each time-point and the data are double-plotted for the homogeneity of the figures.

B. Wild-type mice under constant darkness. CT0 corresponds to the beginning of the constant dark condition.

C. Wild-type mice during food deprivation. RNA from four mice are used for each time-point.

D. *Cry1*/*Cry2* knockout mice under the light-dark cycle. RNA from two mice are used for each time-point and the data are double-plotted for the homogeneity of the figures.

**Figure S4. Activation of the IRE1α pathway by feeding in mouse liver**

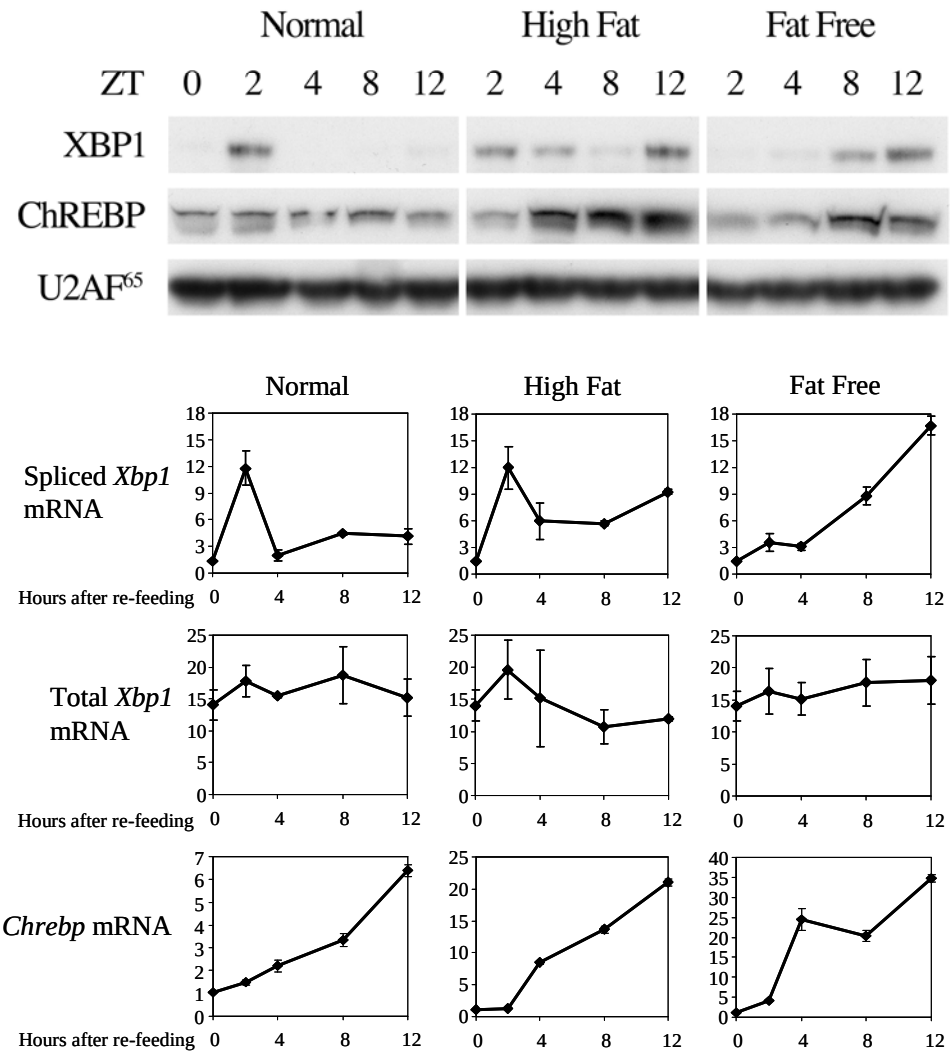


After a complete night of food deprivation, mice were re-fed with normal, high fat or fat free diets. Activation of XBP1 and ChREBP were measured by western blotting (upper panel) or real-time RT-PCR (lower panel) 2, 4, 8 and 12 hours after the start of the re-feeding. If it has been previously shown that feeding activates UPR (Oyadomari et al., 2008), we show here that the composition of the food influences this activation. If normal diet induces a transient and rapid activation of XBP1, high fat diet induces a strong and sustained activation whereas fat free diet caused a delayed but sustained activation correlated with activation of *de novo* synthesis of fatty acid induced by ChREBP activation and translocation in the nucleus (Uyeda and Repa, 2006). The high induction of *Chrebp* mRNA after re-feeding, particularly with high carbohydrate diet, has been previously described (He et al., 2004).

**Figure S5. Rhythmic activation of the IRE1α pathway in *ob*/*ob* mice**

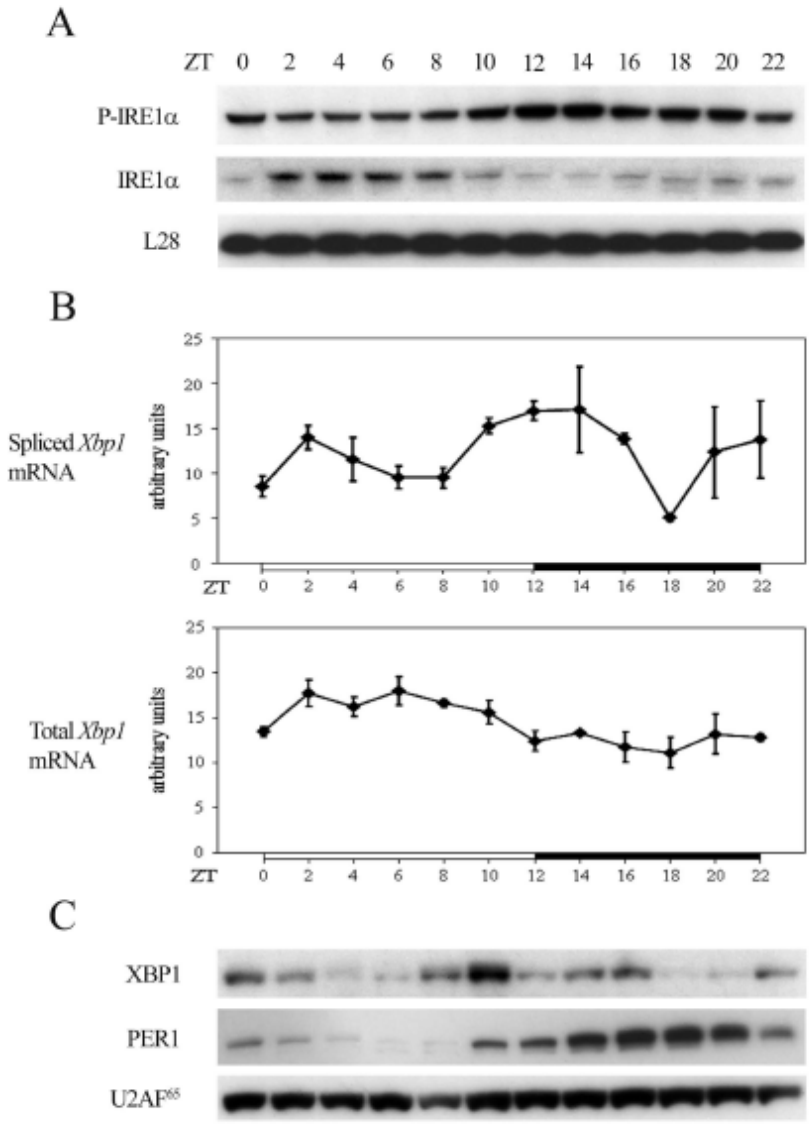


The UPR system has been described highly activated in the liver of obese mice (Ozcan et al., 2004). To see if this high activation disrupts the observed 12-hours period rhythm, we study the UPR temporal activation in the liver of *ob*/*ob* mice. We also found a very high phosphorylation of IRE1α throughout the day, but with a first small peak at ZT0 and a second broad peak from ZT10 to ZT16 (panel A). In the same time, we found the inverse profile for the total IRE1α protein, also probably caused by the degradation of *Ire1α* mRNA by activated IRE1α (Tirasophon et al., 2000). L28 ribosomal protein was given as a loading control. This pattern of activation was also found for the splicing of *Xbp1* mRNA (panel B) and for the accumulation of XBP1 protein in the nucleus (panel C). PER1 accumulation is given as a control for diurnal synchronization of the animals and U2AF$^{65}$ as a loading control. This rhythm is comparable to the rhythm found in wild-type mice,

even if the amplitude seems to be lower. Surprisingly, levels of splicing of *Xbp1* and of XBP1 in the nucleus were equivalent to the ones found in wild-type lean mice. Interestingly, this result was recently confirmed in both *ob*/*ob* and *db*/*db* models of obese mice (Wang et al., 2009) and could reflect an adaptation of the cells to survive to constitutive activation of the UPR (Lin et al., 2007). This result reflects also the fact that phosphorylation of IRE1α at Ser724 did not reflect all the time the real ribonuclease activity of the protein (Sha et al., 2009).

**Figure S6. Rhythmic activation of the IRE1α pathway in *Clock* knockout mice**

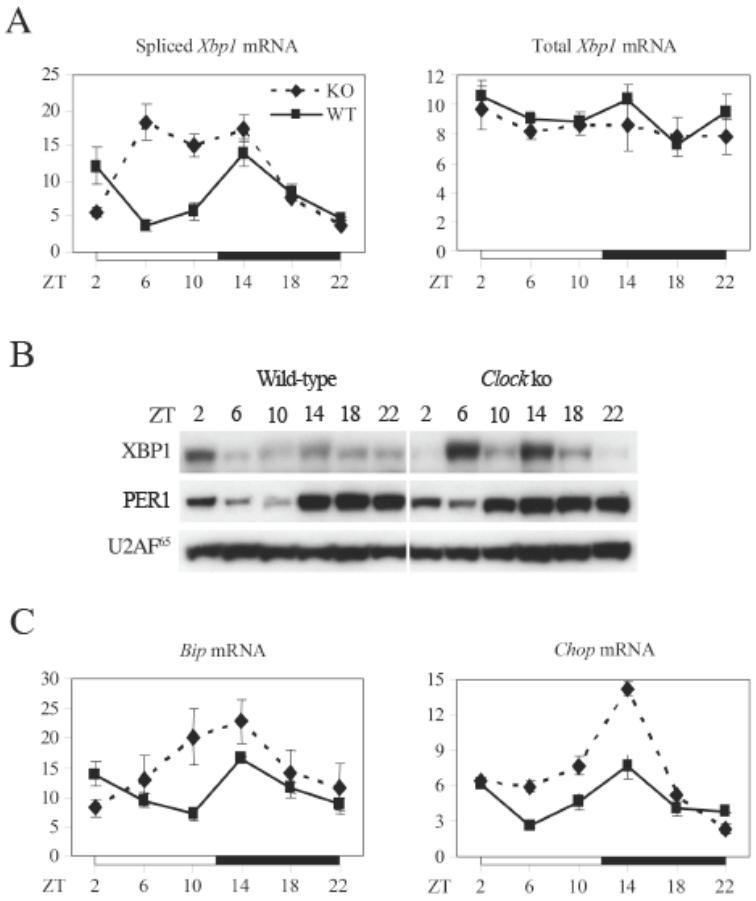


A. Temporal splicing of *Xbp1* mRNA in the liver of wild-type and *Clock* knockout mice. The *Zeitgeber* times (ZT) at which the animals were sacrificed are indicated on the bottom of the figure.

B. Temporal accumulation of XBP1 protein in the liver nucleus of wild-type and *Clock* knockout mice. PER1 accumulation is given as a control for circadian synchronization of the animals and $U2AF^{65}$ as a loading control.

C. Temporal expression of *Bip* and *Chop* mRNA in mouse liver by Real-time RT-PCR.

Interestingly *Clock* knockout mice, which are characterized by a robust circadian behavior despite very low expression of Clock-controlled genes in peripheral tissue and more particularly the PARbZip transcription factor *Dbp* (DeBruyne et al., 2006), present a change in the rhythm of activation of the UPR equivalent to the one found in PARbZip triple knockout mice, but with a broader peak.

**Figure S7. Activation of the IRE1α pathway at CT12 in *Cry1/Cry2* knockout mice kept in constant darkness**

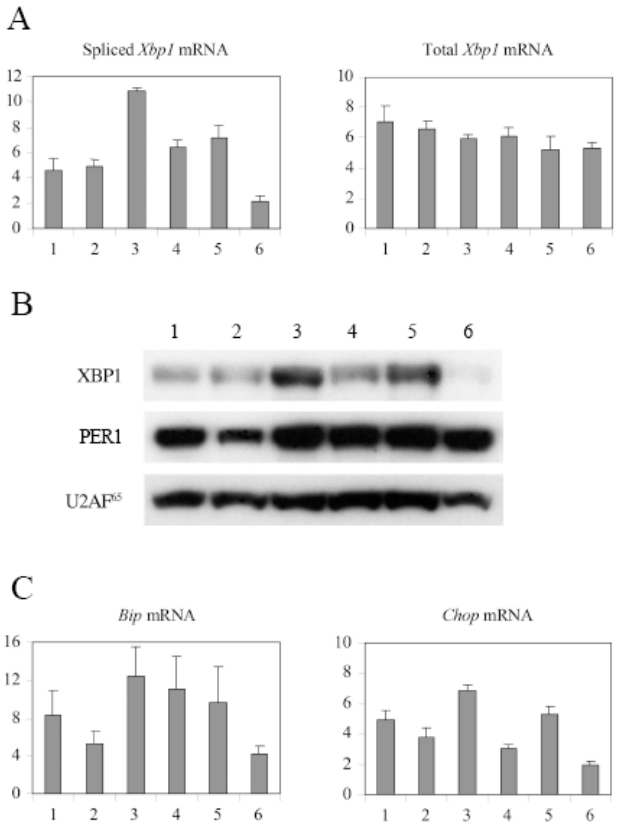


Six *Cry1*/*Cry2* knockout mice were kept in constant darkness for one week and then sacrificed at CT12.

A. Splicing of *Xbp1* mRNA in the liver of 6 individual *Cry1*/*Cry2* knockout mice.

B. Accumulation of XBP1 protein in the liver nucleus of 6 individual *Cry1*/*Cry2* knockout mice. PER1 accumulation is given as a control for the non-circadian synchronization of the animals and $U2AF^{65}$ as a loading control.

C. Expression of *Bip* and *Chop* mRNA in mouse liver of 6 individual *Cry1*/*Cry2* knockout mice by Real-time RT-PCR.

As shown before, feeding induces activation of the UPR in the liver. The *Cry1*/*Cry2* knockout mice present an arrhythmic behavior when they are kept in constant darkness (van der Horst et al., 1999) and, as a consequence, present an arrhythmic feeding behavior in this condition. We thus expected a high degree of variability in the activation of the UPR in constant darkness at CT12, a time when these mice present a high activation in light-dark conditions, probably due to higher food consumption at that time. It is exactly what we observed concerning XBP1 activation and expression of its target genes.

**Figure S8. Physiological parameters of *Cry1*/*Cry2* knockout mice**

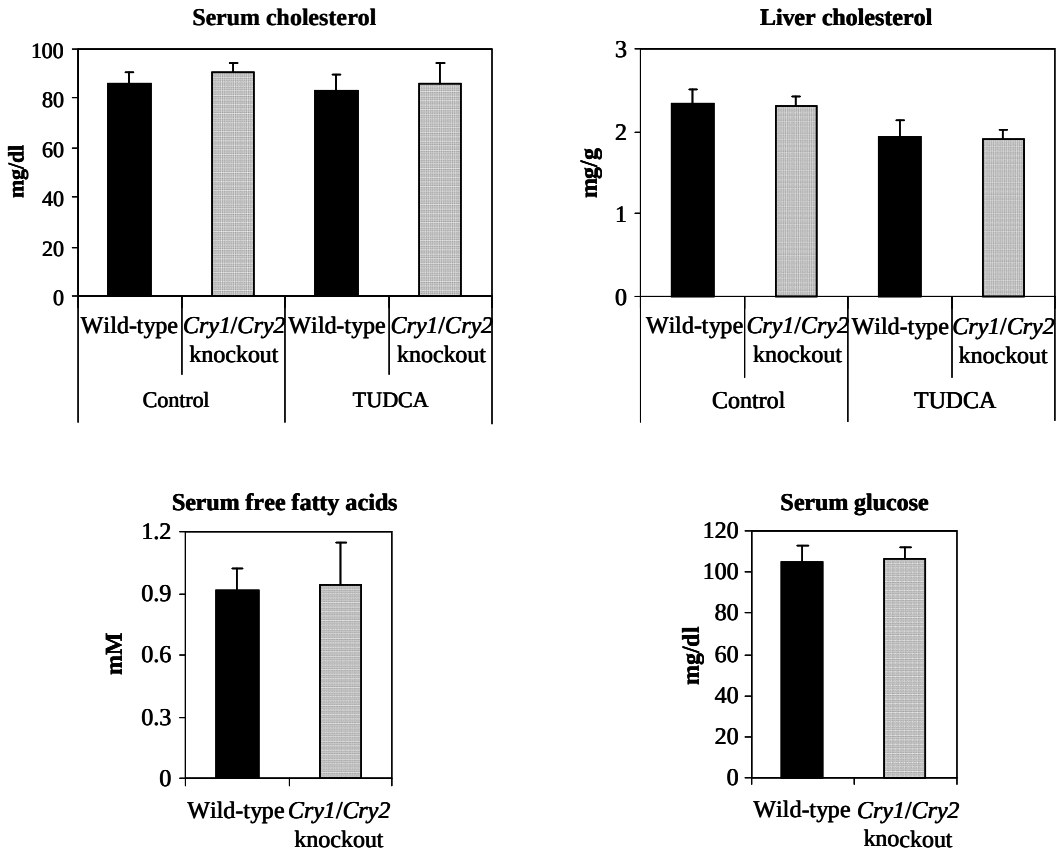


Six male wild-type or *Cry1*/*Cry2* knockout mice were sacrificed at ZT0 after 12 hours of fasting in control conditions or after injection of TUDCA (200 mg/kg) during two weeks. Total cholesterol concentrations in both serum and liver, and free fatty acids and glucose concentration in the serum were measured as described in Experimental procedure. Serum and liver triglycerides concentrations are given on Figure 5. Mean values ± SEM are given. No significant differences were found for serum cholesterol, free fatty acids and glucose concentrations. TUDCA seems to decrease the liver cholesterol concentration on both wild-type and *Cry1*/*Cry2* knockout mice but the difference is not statistically significant.

**Figure S9. Temporal expression of UPR regulated genes and SREBP target genes in *Clock*Δ*19* mutant mice liver**

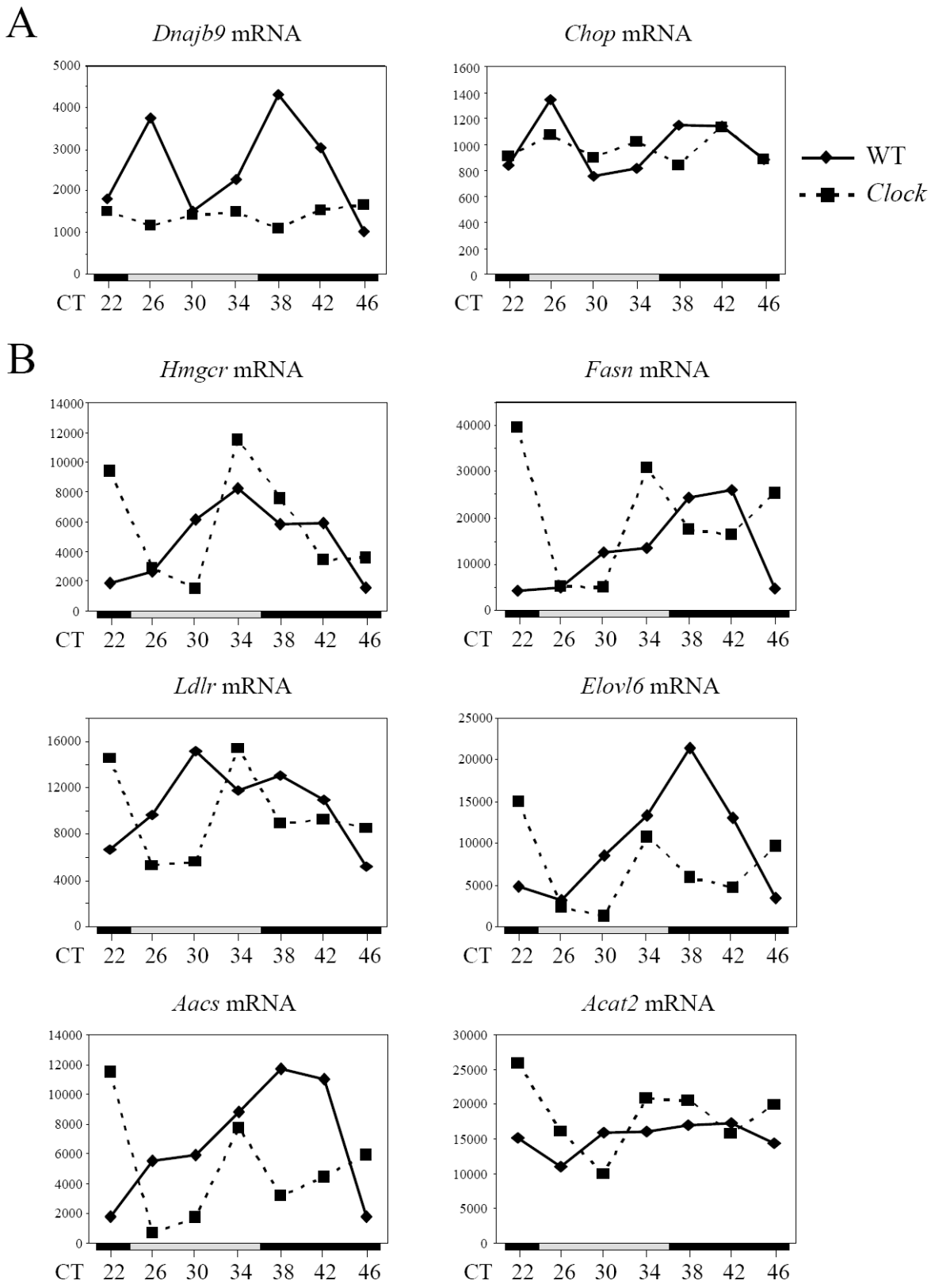

Data from CT 22 to CT 46 on constant dark conditions from wild-type and *Clock∆19* mutant mice published by Miller et al. (2007) were analyzed *post-hoc*. For this, the average values from the two series of data from each condition were calculated. Data for genes regulated during the UPR or regulated by SREBP transcription factors in wild-type and *Clock* mice were extracted and plotted. Expression of UPR regulated genes *Chop* and *Dnajb9* are expressed according to the same ultradian rhythm in the liver of control mice but present a non-rhythmic expression in *Clock∆19* mice (A). This absence of rhythm is probably due to the loss of circadian feeding rhythm in *Clock∆19* mice in the constant dark conditions used for this experiment. In the same time, all the SREBP target genes analyzed changes their apparent circadian expressions in control mice to an ultradian expression in *Clock∆19* mice (B).

## Supplemental experimental procedures

### Mice kept in constant darkness and starvation

For mice kept in constant dark condition, mice were shifted into complete darkness after the last dark period and then sacrificed every two hours during the next 48h. For starvation experiments, mice were deprived from food during one complete night and then during the following 24h mice were sacrificed every two hours.

### Tunicamycin Injections

The drug was injected i.p. at a dose of 1 mg/Kg every 4 hours during 24 hours. 4 hours after injection, mice were sacrificed and livers were rapidly harvested. One part is froozen in liquid nitrogen and kept at -80°C for RNA and total protein extraction, the rest is used for nuclear proteins extraction.

### TUDCA injections

For the injections of Tauroursodeoxycholic acid (TUDCA), the compound (Calbiochem) was solubilised in PBS and injected i.p. every day at ZT6 during 2 weeks at a dose of 200 mg/Kg. At the end of these 2 weeks, the animals were fasted for a complete night (12 hours) and sacrificed at ZT0.

### Animal re-feeding experiment

10 weeks male C57/Bl6 mice were kept in *ad libitum* feeding for one week before the experiment. Animals are then deprived from food for a complete night (the eating period). The following morning, animals were re-feed at ZT0 (when lights turn on) with standard chow (A03) from Safe (Augy, France), high fat (TD.03350) or fat free diets (TD.03314), both from Harlan Teklad. Animals were sacrificed 2, 4, 8 and 12 hours after the beginning of re-feeding.

### *Post hoc* Analysis of microarray data on *Clock* mice

Microarray data from Miller et al. (2007) were downloaded on Gene Expression Omnibus (GEO) database, (accession no. GSE3751). Data from CT 22 to CT 46 on constant dark conditions from wild-type and *Clock* mutant mice were analyzed. For this, the average values from the two series of data from each condition were calculated. Data for genes regulated during the UPR or regulated by SREBP transcription factors (Horton et al., 2003) in wild-type and *Clock* mice were extracted and plotted. Representative data are given on Figure S9.

## Details of the probes used for Northern blotting

| Gene | Reference sequence | Position |
|---|---|---|
| *Bip* | NM_022310.3 | +804 to +1845 |
| *Hrd1* | NM_028769.5 | +453 to +1491 |
| *Dnajb9* | NM_013760.4 | +140 to +788 |
| *Chop* | NM_007837.3 | +163 to +669 |
| *ERp72* | NM_009787.2 | +55 to +1054 |
| *Calr* | NM_007591.3 | +87 to +1149 |
| *Grp58* | NM_007952.2 | +247 to +1302 |
| *Dnajc3* | NM_008929.3 | +256 to +1196 |
| *Sel1h* | NM_011344.2 | +114 to +1225 |
| *Ire1α* | NM_001433.3 | +114 to +3047 |
| *Hmgcr* | NM_008255.2 | +192 to +1195 |
| *Scd1* | NM_009127.4 | +145 to +1212 |
| *Fasn* | NM_007988.3 | +528 to +1457 |
| *Srebp1* | NM_011480.3 | +2055 to +3067 |
| *Srebp2* | NM_033218.1 | +2004 to +3210 |
| *Insig1* | NM_153526.5 | +27 to +858 |
| *Insig2* | NM_133748.1 | +216 to +910 |

## Sequences of the primers used for Real-time RT-PCR

| Gene | Forward primer | Reverse primer |
|---|---|---|
| *Gapdh* | CATGGCCTTCCGTGTTCCTA | CCTGCTTCACCACCTTCTTGA |
| Spliced *Xbp1* | CTGAGTCCGAATCAGGTGCAG | GTCCATGGGAAGATGTTCTGG |
| Total *Xbp1* | TGGCCGGGTCTGCTGAGTCCG | GTCCATGGGAAGATGTTCTGG |
| *Bip* | GAAAGGATGGTTAATGATGCTGAG | GTCTTCAATGTCCGCATCCTG |
| *Chop* | CATACACCACCACACCTGAAAG | CCGTTTCCTAGTTCTTCCTTGC |
| *Hmgcr* | AGCTTGCCCGAATTGTATGTG | TCTGTTGTGAACCATGTGACTTC |
| *Fasn* | GTGTCCAAGAAGTGCAGCAA | GGAGCGCAGGATAGACTCAC |
| *Ldlr* | TGGGCTCCATAGGCTATCTG | GCCACCACATTCTTCAGGTT |
| *Elovl6* | TGCCATGTTCATCACCTTGT | TACTCAGCCTTCGTGGCTTT |
| *Cyp2b10* | CGCATGGAGAAGGAGAAGTC | GGTGCCGACAAAGAAGAGAG |
| *Chrebp* | CTGGGGACCTAAACAGGAGC | GAAGCCACCCTATAGCTCCC |

## References of the antibodies used for Western blotting

| Protein | Reference | Company |
|---|---|---|
| XBP1 | sc-7160 | Santa Cruz Biotechnology |
| IRE1α | sc-20790 | Santa Cruz Biotechnology |
| ATF6α | sc-22799 | Santa Cruz Biotechnology |
| CHOP | sc-793 | Santa Cruz Biotechnology |
| SREBP2 | sc-5603 | Santa Cruz Biotechnology |
| INSIG2 | sc-66936 | Santa Cruz Biotechnology |
| L28 Ribosomal protein | sc-50362 | Santa Cruz Biotechnology |
| SREBP1 | NB100-2215SS | Novus Biologicals |
| INSIG1 | NB110-55244SS | Novus Biologicals |
| ChREBP | NB400-135 | Novus Biologicals |
| SCD1 | 2794 | Cell Signaling Technology |
| FASN | 3180 | Cell Signaling Technology |
| P-IRE1 (Ser 724) | ab48187 | Abcam |
| HMGCR | 07-457 | Millipore |
| $U2AF^{65}$ | U4758 | Sigma |
| PER1 | Brown et al., 2005 | |

## References


Brown, S.A., Ripperger, J., Kadener, S., Fleury-Olela, F., Vilbois, F., Rosbash, M., and Schibler, U. (2005). PERIOD1-Associated Proteins Modulate the Negative Limb of the Mammalian Circadian Oscillator. Science 308, 693-696.

DeBruyne, J.P., Noton, E., Lambert, C.M., Maywood, E.S., Weaver, D.R., and Reppert, S.M. (2006). A Clock Shock: Mouse CLOCK Is Not Required for Circadian Oscillator Function. Neuron 50, 465-477.

He, Z., Jiang, T., Wang, Z., Levi, M., and Li, J. (2004). Modulation of carbohydrate response element-binding protein gene expression in 3T3-L1 adipocytes and rat adipose tissue. Am J Physiol Endocrinol Metab 287, E424-430.

Horton, J.D., Shah, N.A., Warrington, J.A., Anderson, N.N., Park, S.W., Brown, M.S., and Goldstein, J.L. (2003). Combined analysis of oligonucleotide microarray data from transgenic and knockout mice identifies direct SREBP target genes. Proc Natl Acad Sci U S A. 100, 12027-12032.

Lin, J.H., Li, H., Yasumura, D., Cohen, H.R., Zhang, C., Panning, B., Shokat, K.M., LaVail, M.M., and Walter, P. (2007). IRE1 Signaling Affects Cell Fate During the Unfolded Protein Response. Science 318, 944-949.

Miller, B.H., McDearmon, E.L., Panda, S., Hayes, K.R., Zhang, J., Andrews, J.L., Antoch, M.P., Walker, J.R., Esser, K.A., Hogenesch, J.B., and Takahashi, J.S. (2007). Circadian and CLOCK-controlled regulation of the mouse transcriptome and cell proliferation. Proc Natl Acad Sci U S A. 104, 3342-3347.

Oyadomari, S., Harding, H.P., Zhang, Y., Oyadomari, M., and Ron, D. (2008). Dephosphorylation of Translation Initiation Factor 2α Enhances Glucose Tolerance and Attenuates Hepatosteatosis in Mice. Cell Metab. 7, 520-532.

Ozcan, U., Cao, Q., Yilmaz, E., Lee, A.-H., Iwakoshi, N.N., Ozdelen, E., Tuncman, G., Gorgun, C., Glimcher, L.H., and Hotamisligil, G.S. (2004). Endoplasmic Reticulum Stress Links Obesity, Insulin Action, and Type 2 Diabetes. Science 306, 457-461.

Rutkowski, D.T., Wu, J., Back, S.-H., Callaghan, M.U., Ferris, S.P., Iqbal, J., Clark, R., Miao, H., Hassler, J.R., Fornek, J., Katze, M.G., Hussain, M.M., Song, B., Swathirajan, J., Wang, J., Yau, G.D.Y., and Kaufman,

R.J. (2008). UPR Pathways Combine to Prevent Hepatic Steatosis Caused by ER Stress-Mediated Suppression of Transcriptional Master Regulators. Dev Cell 15, 829-840.

Sha, H., He, Y., Chen, H., Wang, C., Zenno, A., Shi, H., Yang, X., Zhang, X., and Qi, L. (2009). The IRE1α-XBP1 Pathway of the Unfolded Protein Response Is Required for Adipogenesis. Cell Metab. 9, 556-564.

Tirasophon, W., Lee, K., Callaghan, B., Welihinda, A., and Kaufman, R.J. (2000). The endoribonuclease activity of mammalian IRE1 autoregulates its mRNA and is required for the unfolded protein response. Genes Dev. 14, 2725-2736.

Uyeda, K., and Repa, J.J. (2006). Carbohydrate response element binding protein, ChREBP, a transcription factor coupling hepatic glucose utilization and lipid synthesis. Cell Metab. 4, 107-110.

van der Horst, G.T.J., Muijtjens, M., Kobayashi, K., Takano, R., Kanno, S.-i., Takao, M., de Wit, J., Verkerk, A., Eker, A.P.M., van Leenen, D., Buijs, R., Bootsma, D., Hoeijmakers, J.H.J., and Yasui, A. (1999). Mammalian Cry1 and Cry2 are essential for maintenance of circadian rhythms. Nature 398, 627-630.

Wang, Y., Vera, L., Fischer, W.H., and Montminy, M. (2009). The CREB coactivator CRTC2 links hepatic ER stress and fasting gluconeogenesis. Nature 460, 534-537.